

Coordinates

Volume XXI, Issue 8, August 2025

THE MONTHLY MAGAZINE ON POSITIONING, NAVIGATION AND BEYOND

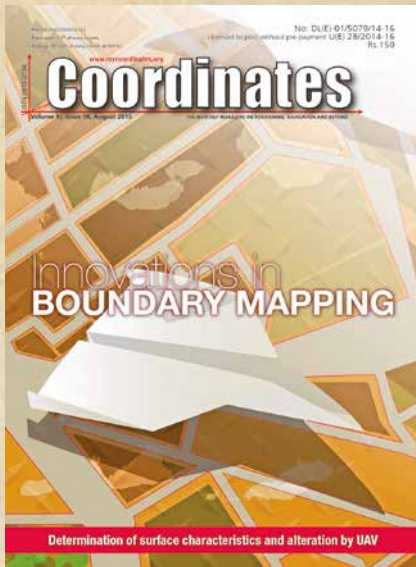
Educating primary
school students about
Surveying



Solar radio bursts impact on the International GNSS Service
Network during Solar Cycle 24

In Coordinates

10 years before...



mycoordinates.org/vol-XI-issue-08-August-2015

Multi-Constellation GNSS based on next generation RAIM

Mikael Mabilieu, Jonathan Vuillaume, Gerhard Berz, Focal Point, Navigation Infrastructure, CNS project Engineer, Engineer, Egis, EUROCONTROL, and Technical Advisor, the Egis Avia, France Avia, France ICAO Navigation Systems Panel, Belgium

Pr Igor Nikiforov, Professor, University of Technology of Troyes, Charles Delaunay Institute, Troyes, France

Okko F Bleeker, Director, Research and Development, Europe, Rockwell Collins

An extensive analysis of the H-ARAIM performance has been provided in this paper showing that ARAIM is robust to the loss of frequency and can provide 100 % availability for LNAV, RNP01 NM operation, US and EU ADS-B mandates in conservative assumptions for URA, Psat and Pconst. In nominal mode of operation based on optimal 24 + 24 satellites constellations, ARAIM can sustain HPL requirements of 20 m.

Innovations in boundary mapping

Mukendwa Mumbone, Ministry of Land Reform, Namibia
Rohan Bennett, University of Twente, The Netherlands

Markus Gerke, University of Twente, The Netherlands
Walter Volkmann, Micro Aerial Projects LLC, USA

This study concludes that the UAV enabled mapping approach enables capture of high resolution images out of which good quality orthophotos can easily be generated. Due to the high resolution nature and timeliness, such images can easily be used for mapping customary land rights boundaries; this can be done in a fast and relatively cheap fashion of vectorising parcels straight on-screen, without having to print the orthophoto.

Determination of surface characteristics and alteration of Koru mining area by UAV photogrammetry

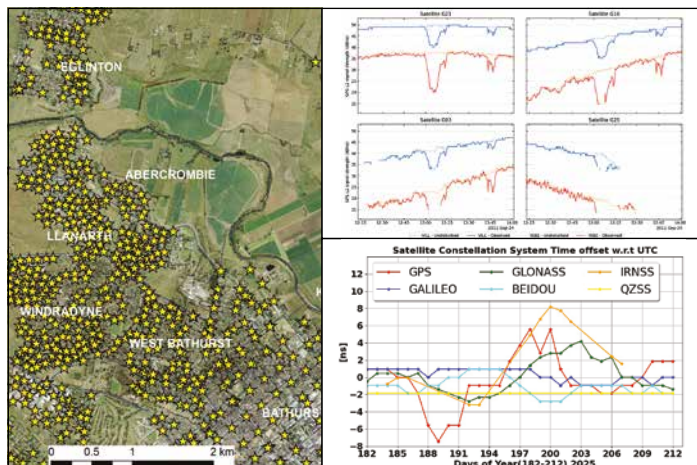
Oya Erenoglu, R Cuneyt Erenoglu and Ozgun Akcay
Department of Geomatics Engineering, Canakkale Onsekiz Mart University, Canakkale, Turkey

In this study, for surface characterization, we showed that a low-cost UAV-based remote sensing approach reveals high-resolution digital surface models. To do it, terrestrial and aerial photographs were taken and their RGB values were compared with each other. Finally, the matched areas, e.g., rhyolitic lava, andesitic lava and rhyolitic tuff were successfully determined, classified and zoned.

Enabling Technology for Citizen and Community Tenure Rights Protection

Neil Pullar, Andrew McDowell and MariaPaola Rizzo
Food and Agriculture Organization of the United Nations, Rome

The full potential of open source software application on mobile devices to address tenure related needs has a long way to go before it has been fully explored. Astute land administration practitioners in as diverse countries as Nigeria, Vietnam and Afghanistan have seen or heard of Open Tenure and despite its initial focus on community recording of tenure relationships have quickly seen its potential for use in a range of land administration field activities.



In this issue

Coordinates Volume 21, Issue 8, August 2025

Articles

Educating primary school students about surveying VOLKER JANSSEN 5 **Solar radio bursts impact on the International GNSS Service Network during Solar Cycle 24** MANUEL FLORES-SORIANO 11 **GNSS Constellation Specific Monthly Analysis Summary: July 2025** NARAYAN DHITAL 25

Columns

Old Coordinates 2 **My Coordinates** EDITORIAL 4 **News** GNSS 30 IMAGING 31 UAV 32 INDUSTRY 32 **Mark Your Calendar** 34

This issue has been made possible by the support and good wishes of the following individuals and companies
Manuel Flores-Soriano, Narayan Dhital and Volker Janssen; SBG System, and many others.

Mailing Address

A 002, Mansara Apartments
C 9, Vasundhara Enclave
Delhi 110 096, India.
Phones +91 11 42153861, 98102 33422, 98107 24567

Email

[information] talktous@mycoordinates.org
[editorial] bal@mycoordinates.org
[advertising] sam@mycoordinates.org
[subscriptions] iwant@mycoordinates.org

Web www.mycoordinates.org

Coordinates is an initiative of CMPL that aims to broaden the scope of positioning, navigation and related technologies. CMPL does not necessarily subscribe to the views expressed by the authors in this magazine and may not be held liable for any losses caused directly or indirectly due to the information provided herein. © CMPL, 2025. Reprinting with permission is encouraged; contact the editor for details.

Annual subscription (12 issues)
[India] Rs.1,800* [Overseas] US\$100*

*Excluding postage and handling charges

Printed and published by Sanjay Malaviya on behalf of Coordinates Media Pvt Ltd

Published at A 002 Mansara Apartments, Vasundhara Enclave, Delhi 110096, India.

Printed at Thomson Press (India) Ltd, Mathura Road, Faridabad, India

Editor Bal Krishna

Owner Coordinates Media Pvt Ltd (CMPL)

This issue of Coordinates is of 36 pages, including cover.

Climate Insight

NASA's OCO-2 and OCO-3 satellites orbit tirelessly,
Monitoring carbon dioxide levels with remarkable precision,
Mapping emissions and absorptions across the globe.
Launched in 2014 and 2019,
These missions faces sudden termination,
As Trump's 2026 budget proposal slashes their funding.
This may cripple climate research,
Hindering data on greenhouse gases and global warming trends.
This is a disturbing development,
When farmers grapple with unpredictable droughts,
Cities face deluges, hurricanes grow fiercer, rising sea level, ...
These satellites are critical in predicting and mitigating crises.
It is the time to double down on these assets,
Not discard them.

Bal Krishna, Editor
bal@mycoordinates.org

ADVISORS Naser El-Sheimy PEng, CRC Professor, Department of Geomatics Engineering, The University of Calgary Canada, George Cho Professor in GIS and the Law, University of Canberra, Australia, Professor Abbas Rajabifard Director, Centre for SDI and Land Administration, University of Melbourne, Australia, Luiz Paulo Souto Fortes PhD Associate Professor, University of State of Rio Janeiro (UERJ), Brazil, John Hannah Professor, School of Surveying, University of Otago, New Zealand

Educating primary school students about surveying

This paper presents an innovative initiative to engage primary school students (and their parents) with surveying in a way that is both educational and fun, while also delivering real-world benefits to the surveying profession.



Dr Volker Janssen
Geodetic Surveyor in
the Geodesy & State
Adjustment team at
DCS Spatial Services,
NSW Department of
Customer Service, in
Bathurst, Australia.

Surveying is a unique and rewarding career that enables exposure to cutting-edge technology, involves conducting detective work in the field and significantly contributes to society. While surveying offers great job prospects with the opportunity to specialise in numerous areas, it is plagued by a notorious skills shortage and continuing problems to attract enough tertiary students to feed demand. The ageing demographic of the existing workforce and a lack of diversity within the profession only exacerbate these woes (Underwood and Powell, 2019; Cripps and Fairlie, 2024).

While the surveying profession has a long history of evolving and adapting to inevitable change driven by political, economic and technological factors (e.g. Enemark, 2009; Staiger, 2023), sometimes there is stubborn refusal to acknowledge that change is both inevitable and continuous. To stay relevant in an era of non-skilled users increasingly capturing geospatial data, the profession must identify innovative ways to add value to measurement and geospatial data and then promote this value within society to raise the public profile of the surveyor (Underwood and Powell, 2019).

Promotion of the profession to school aged students provides surveying exposure to a wide audience and helps develop a pipeline of future surveyors. Over the years, many initiatives have tried to attract young people into surveying. For example, in Australia, the Surveying Taskforce was created to help combat the current shortfall of surveyors. It set up a website to capture those considering a career in surveying,

has a social media presence and provides resources for presentations to school aged students (Surveying Taskforce, 2020). Surveyors can become a 'surveying ambassador', which provides opportunities to be involved in career events, school presentations, assisting with information days or hosting work experience students.

The 'Get Kids into Survey' campaign, developed in the UK, offers resources such as surveying-themed colouring sheets, activity posters, homework projects and the Geo Squad comic (Ball, 2025). Again, engagement of the profession is sought via ambassadors and sponsors to utilise the available resources and reach the target audience.

Similarly, the UK Ordnance Survey (OS) gives away free maps to 11-year-olds through their schools (Owen, 2007). Each year 7 pupil in England, Scotland and Wales receives a free 1:25,000 scale OS Explorer map of their local area, resulting in more than 700,000 maps being distributed through schools every year. It now produces special paper and wall maps centred on the schools, helping children to learn geography in their own backyard and that all-important sense of direction.

At the university level, efforts have been undertaken to modernise the curriculum and increase student intake in various ways (e.g. Enemark, 2009; Roberts, 2016; Roberts and Harvey, 2019). Furthermore, the use of humour can improve student learning and help convey scientific information to a much wider and more general audience (e.g. Janssen, 2012, 2019, 2023; McAlister

and Hill, 2023). While many of these initiatives have been successful, unfortunately the problem persists with the capability gap in Australia reaching 1,500 surveying professionals in 2023/24 as new supply from graduates falls short of the increased demand (Consulting Surveyors National, 2023).

Consequently, the education of the public and the continued promotion of the surveying profession is the responsibility of all surveyors. This paper presents an innovative initiative to engage primary school students (and their parents) with surveying in a way that is educational, healthy and fun, while also delivering real-world benefits to the surveying profession in New South Wales (NSW), Australia.

Background

DCS Spatial Services, a unit of the NSW Department of Customer Service (DCS), is responsible for the maintenance and improvement of the NSW survey

control network, made available to users via the Survey Control Information Management System (SCIMS). SCIMS is the state’s database containing more than 250,000 survey marks on public record, including coordinates, heights, accuracy classifications and other metadata.


When the COVID-19 pandemic was raging in 2020/21, people around the world had to juggle working from home, childcare, child education and entertainment, all while observing the lockdown restrictions in force to combat the coronavirus outbreak. During these challenging times, the author introduced his then 8-year-old daughter to a new game: ‘SSM spotting’. This was explained as combining a treasure hunt with the ‘Spotto’ game (spot a yellow car on the road and the first person to call out ‘Spotto’ claims the point). It included walking around the neighbourhood (exercise and mental health benefits, while practising a sense of direction) and looking for survey marks along the way (entertainment). This could also be thought of as a very specific form of geocaching.

We found many interesting types of survey marks (education): nails, drill hole and wings, survey pegs, Permanent Mark (PM) cover boxes (often with dots of yellow paint on power poles or fence posts providing clues to their location) and, of course, many State Survey Marks (SSMs) located along the kerb. We intentionally avoided those survey marks (PMs) that were placed in cover boxes (cast steel box with liftable lid) to avoid digging and any ants or spiders hiding under the lid.


The author took photos of all the SSMs we came across, often with his daughter performing handstands, bridges or the splits while pointing to the mark (exercise and entertainment) (Figure 1). In total, 70 SSMs were photographed, and the images added to the DCS Spatial Services archive. Later, SCIMS was updated with metadata related to these survey marks to improve the information held on public record (innovation and customer service). Note the use of a bucket hat to provide sun protection and to help make the photographed subject more anonymous.




Figure 1: Examples of SSM spotting images (the colourful water bottle is used to easily identify the mark location).



SSM Spotting Activity





Our Stage 3 students have started a new activity to learn about State Survey Marks (SSMs), which can be found along the kerb of roads across the entire state. Each student is asked to find, inspect and photograph three SSMs around where they live or anywhere else they would like to go for a walk with their parent or carer. Instructions and background information have been distributed to students via Google classroom. Please support this worthwhile activity. We are planning to get Stage 2 students involved next term.




Figure 2: Promoting the SSM spotting activity in the school's newsletter.

Primary school activity

Bathurst South Public School is a primary school educating about 220 students from kindergarten through to year 6. In late 2021, the author approached the school's principal with a proposal to introduce SSM spotting as an activity that not only ticks the boxes of education, exercise and mental health, but also promotes community engagement. The aim was to engage students (and their parents or carers) with surveying and encourage them to view their surroundings a little differently (most people are oblivious to survey marks), while producing rewarding outcomes that are used by the NSW Government and the surveying profession in the real world.

The proposal was met with considerable support and enthusiasm, and it was decided to trial the activity in a single year 5/6 class in 2022. After completing the mandatory Working with Children Check, the author gave a presentation to introduce the activity, followed by a practical demonstration at two survey marks in front of the school. Soon after, a class excursion was organised where students would take turns in finding, checking and photographing survey marks while walking along residential streets surrounding the school. The excursion was well received by the students who were eager to participate in this peculiar treasure hunt.

During this time, relevant documentation and processes were refined based on the experience gained and any feedback received. This included considering the following concerns:

- Road safety: Students and their parents/carers will be used to walking on the footpaths along their local roads together, so this should not be an issue. If their residence is along a busy road, they should select a quieter area for this activity.
- Wheelchair access: Footpaths suitable for wheelchairs are available in various parts of town, providing safe access to survey marks.
- Children in photos: Parents/carers need

to be made aware that the photos taken of the survey marks will be included in the NSW Government's archive of survey mark photos. Having their children shown in the photos is optional and not necessarily encouraged.

- Privacy: The names of participating students are not disclosed to DCS Spatial Services. Any file or folder names including personal information are anonymised before being passed on.
- Work Health and Safety (WHS): The activity was assessed and conducted under the school's WHS policies and insurances.

Due to the packed curriculum and other school activities taking priority, it took another year until SSM spotting was rolled out across all stage 3 (year 5 & 6) classes in 2023. Again, this was accompanied by a

presentation and practical demonstration. The activity was also promoted in two issues of the weekly newsletter distributed to students and their families (Figure 2).

Instructions for students

Background information and instructions provided in written form and during the presentation and demonstration sessions purposely used language appropriate to the target audience. It was explained that surveyors are experts at knowing their location or position. They measure angles, distances, height differences and positions to determine where things are and how they relate to each other. Students were introduced to different types of survey marks (and their purpose) and informed that the data collected



Figure 3: Photos taken at SS77027, showing a close-up of the SSM plaque and views from four perpendicular directions, using the kerb for orientation.

will be used by the NSW Government for the benefit of the community.

In summary, the instructions included:

- Take a parent/carer for a walk in the neighbourhood and find at least three SSMs located along the kerb of the road.
- Inspect the survey mark, brush off dust if required, and write its number and health status (stable, unstable or damaged) on a notepad.
- Take up to five photos in landscape format, including a close-up of the mark itself showing its number plate and (if possible and safe to do so) a photo from each of four perpendicular directions showing the mark and any background.
- Move clockwise around the mark when taking photos and place a colourful water bottle next to the mark, so it can easily be identified in the photos (Figure 3).
- Take a photo of the simple list showing the marks spotted and their health status.
- Download the photos and rename them, so we can easily see which photo belongs to which survey mark and when it was taken (e.g. *SS123456_20230413_1.jpg* and *SSM_health.jpg*).
- Organise the files into folders and upload them to the school.
- How to use the free NSW Survey Marks smartphone app to explore survey marks further or get some clues about where to find them.
- How to use the sketch plan like a treasure map to find the survey mark.
- What to bring and how to be safe.

The uploaded files were checked (and anonymised if required) by the school and passed on to the author at DCS Spatial Services. Data management then included ensuring correct file naming, selecting the preferred set of photographs for marks spotted by multiple students and assessing the health status of each mark based on the photographs and the students' comments. A tally was kept, documenting the spotted marks and including relevant metadata required for the integration

of this information into DCS Spatial Services databases and archives.

Results

The SSM spotting activity at Bathurst South Public School resulted in 275 survey marks (including 25 PMs) being spotted, photographed and then updated in SCIMS. The photos have been added to the DCS Spatial Services archive, significantly increasing the number of survey marks with available images in Bathurst (Figure 4). In the future, these photos may be made available to surveyors via a modernised SCIMS to assist them in survey planning, e.g. in determining whether a particular survey mark is affected by tree cover or other obstructions (negatively affecting satellite-based positioning) or whether an instrument can be set up on the mark safely and with minimal disruption to traffic. To this end, blur filters may be applied to protect the privacy of any persons in the photos if required.

The SCIMS metadata update included specifying the mark status (generally 'found intact') with a corresponding comment and date, along with specifying (or confirming) the mark type and entering (or confirming) information about who placed the mark and when it was placed by interrogating the locality sketch plan on public record (Janssen, 2025). For PMs, the height of the mark below/above ground level was also measured and archived (for SSMs this value was generally zero).

Some survey marks were found damaged or in need of repair.

The students' notes on the health status of each mark in conjunction with the close-up photos taken were crucial in ascertaining whether repair work was required. For example, DCS Spatial Services performed repairs in cases where the SSM brass plaque was wobbling in the concrete, removable from the kerb, buried by recently added bitumen or where part of the mark number had been rubbed out. Some PMs were also repaired to allow easy opening and closing of the cover box, and to remove trip hazards caused by stuck or missing lids. On one occasion, a cover box that had been pushed off the mark and thereby prevented the survey mark from being occupied was re-centred, enabling it to return to service.

Challenges

While these results are very pleasing and encouraging, several challenges were encountered. Despite the considerable support and enthusiasm shown by the

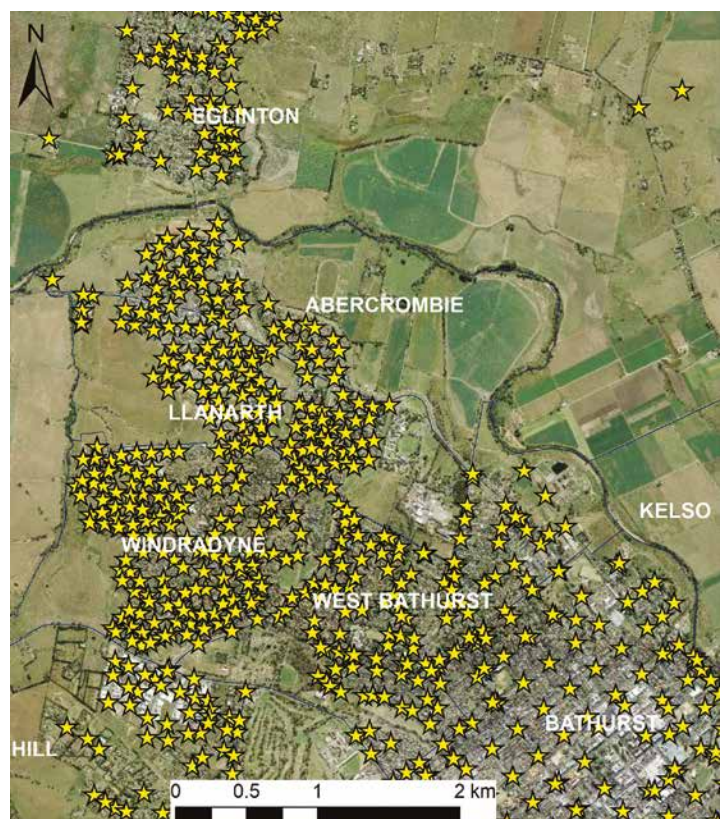


Figure 4: Aerial map of Bathurst suburbs, indicating survey marks with images archived in the DCS Spatial Services database.

school, it proved difficult to include the SSM spotting activity in an already packed curriculum. This caused the activity to be drawn out over two school years, which may have negatively affected the interest and enthusiasm shown by the students involved in the initial pilot. Like homework, the activity was not compulsory (or not promoted as such). Unfortunately, it was not possible to include SSM spotting as an option in the suggested homework roster distributed to students for the school term. For this cohort, the activity relied on parental supervision, and parents/carers may have been more inclined to partake or adequately prepare for the activity if it were perceived as compulsory.

While there was a lot of interest among students, particularly during the very successful class excursion, only a few students followed through with the entire activity in their own time afterwards. Several students reported spotting survey marks but not taking any photos at the time or taking some photos but not uploading them to the school. The offer to help with the downloading and renaming of images in the school's computer lab was not taken up. Consequently, most marks were completed by only a few students, mainly by the author's daughter (who, understandably, became less enthusiastic as time went on). Asking a few school friends to come along increased the fun factor and extended the duration of participating in the activity. Towards the end, the author embarked on a couple of solo trips to capture the remaining survey marks in a particular area.

The SSM spotting activity attracted the attention of concerned residents on social media. A local neighbourhood group lit up with posts pertaining to a strange person walking around the streets, apparently taking photos of his water bottle sitting on the gutter, sometimes while children are posing in the photos. While some posts were concerned about the person's mental wellbeing, others speculated that he may

have a more sinister motive and was actually taking photos of people's houses to discover whether CCTV cameras are installed. The mystery was eventually solved through an explanatory post by one of the author's colleagues. A few residents made the effort to say hello to the strange person walking the streets and were promptly informed of the school activity taking place.

Potential extensions and future activities

SSM spotting can be adapted to students at high school, Vocational Education and Training (VET) institutions (such as TAFE in Australia) and university. High school students may be more suited than primary school students as they are more independent and potentially more interested in following through depending on possible job interests.

As a potential extra relating to spatial awareness, students could be asked to draw or produce a treasure or mud map of the roads searched for survey marks, indicating where each SSM was found with a symbol, labelling them accordingly and including a north arrow. For older kids, the activity could be modified by first checking SCIMS (via the NSW Survey Marks app) for suitable survey marks to track down, similar to geocaching. In urban areas, it could be expanded to include PMs in the footpath, provided the appropriate tools are carried and WHS measures are in place (e.g. including a large screwdriver to open the cover box, a glove for protection from animals and to scoop out dirt, and a measuring tape to determine the mark-to-ground-level height).

From high-school age onwards, students could be asked to measure coordinates with a smartphone or handheld Global Navigation Satellite System (GNSS) unit and create a map with an open-source Geographic Information System (GIS) package like QGIS. This progression from treasure hunt to taking simple measurements not only

increases the activity's challenge and complexity but also allows an introduction to coordinate types and systems.

Students starting a VET or university course in surveying could benefit from SSM spotting as an activity to get a better understanding of the different types of survey marks and their importance, along with exposure to the NSW Survey Marks app, SCIMS and the role of state government in maintaining the state's survey infrastructure. Searching for, identifying and photographing survey marks and updating their metadata could be a useful hands-on practical field exercise. Students could be required to identify a variety of survey marks (cadastral and survey control), including examples of 'found', 'uncertain' and 'destroyed' marks, and use the app to submit updated metadata. In addition, they could load these as a layer in a GIS and be required to find marks not previously visited by other students.

The wider profession could also be involved in SSM spotting, e.g. while contributing to a worthy cause. STEPtember is a global health and wellness fundraising event supporting life-changing cerebral palsy research. It encourages participants of all fitness and ability levels to take part in more than 40 activities to complete a daily target of 10,000 steps. The author encourages the wider profession to mimic the primary school students and find as many survey marks as possible, while staying healthy and supporting a worthy cause.

The NSW Survey Marks app has the potential of being an important tool to help engage students and potentially foster citizen science if it is desired to target an even wider audience (such as the geocaching community). Via its report function, the app can be used by any person to easily upload photos and report on the health status of a survey mark. However, it should be noted that this provides a direct conduit to DCS Spatial Services rather than utilising a moderator as may be desired for a school or tertiary education project to avoid duplication.

Conclusion

This paper has introduced an innovative initiative to engage primary school students (and their parents) with surveying in a way that is educational, healthy and fun, while also delivering real-world benefits to the surveying profession. Students were asked to take their parents/carers for a walk, find SSMs located along the kerb, investigate each mark's health status, take photographs, organise the images, and then upload the data to the school.

At Bathurst South Public School, the SSM spotting activity resulted in 275 survey marks being spotted and photographed. Associated metadata was then updated on public record, and the photos have been added to the DCS Spatial Services archive. This has helped to maintain the NSW survey control network for the benefit of the profession and the wider community. Some survey marks were reported by the students as damaged or in need of repair, prompting DCS Spatial Services to perform repair work as required.

While several challenges were encountered, SSM spotting has successfully educated primary school students and their parents/carers about surveying and provided them with a glimpse into the work of a surveyor. The activity can easily be adapted to cater for high school or tertiary students and has the potential to target citizen science or fundraising activities. It is hoped that this will help in the quest to educate the general public about what surveyors do, raise the profession's public profile and result in more people choosing a career as a surveyor or geospatial professional.

Acknowledgements

Principal Greg Cross and his teaching staff at Bathurst South Public School (particularly Peta Connell, Rachel Vickery and David Prior) are gratefully acknowledged for their support and enthusiasm during the implementation of this school activity. Les Gardner, Senior Surveyor at DCS Spatial Services, is

thanked for embracing the activity while walking his dog around various parts of Bathurst and thereby committing many additional survey mark images to our database. This paper is dedicated to my father, Bernd Janssen, on his 85th birthday. Now a retired registered land surveyor, he was instrumental in engaging me with this wonderful profession of ours – love you, Dad.

References

- Ball E. (2025) Get kids into survey, <https://www.getkidsintosurvey.com/> (accessed July 2025).
- Consulting Surveyors National (2023) Determining the future demand, supply and skills gap for surveying and geospatial professionals: 2022-2032, <http://www.consultingsurveyors.com.au/public/115/files/Our%20Industry/Research/Demand%20Study%20web%20version.pdf> (accessed July 2025).
- Cripps A. and Fairlie K. (2024) How effective are initiatives to recruit women into surveying? *Proceedings of FIG Working Week 2024*, Accra, Ghana, 19-24 May, 18pp.
- Enemark S. (2009) Surveying education: Facing the challenges of the future, *Proceedings of FIG Commission 2 Workshop*, Vienna, Austria, 26-28 February, 11pp.
- Janssen V. (2012) Indirect tracking of drop bears using GNSS technology, *Australian Geographer*, 43(4), 445-452.
- Janssen V. (2019) Let there be rock: The AC/DC phenomenon, *Proceedings of Association of Public Authority Surveyors Conference (APAS2019)*, Pokolbin, Australia, 1-3 April, 106-125.
- Janssen V. (2023) Amusing research in surveying and spatial science, *Proceedings of Association of Public Authority Surveyors Conference (APAS2023)*, Coffs Harbour, Australia, 20-22 March, 3-25.
- Janssen V. (2025) Engaging primary school students (and their parents) with surveying, *Proceedings of FIG Working Week 2025*, Brisbane, Australia, 6-10 April, 15pp.
- McAlister C. and Hills C. (2023) Don't feed cheese to lactose intolerant volcano gods, *Proceedings of Association of Public Authority Surveyors Conference (APAS2023)*, Coffs Harbour, Australia, 20-22 March, 26-36.
- Owen E. (2007) Ordnance Survey's free maps for 11 year olds scheme, *The Cartographic Journal*, 44(2), 101-110.
- Roberts C. (2016) Aspiring beyond UNSW: Connecting students to industry, *Proceedings of Association of Public Authority Surveyors Conference (APAS2016)*, Leura, Australia, 4-6 April, 3-9.
- Roberts C. and Harvey B. (2019) The critical importance of practical exercises in a modern surveying curriculum, *Proceedings of Association of Public Authority Surveyors Conference (APAS2019)*, Pokolbin, Australia, 1-3 April, 139-151.
- Staiger R. (2023) The surveyor 4.0: Which technical skills are needed today? *GIM International*, 37(1), 22-25.
- Surveying Taskforce (2020) A life without limits, <https://www.alifewithoutlimits.com.au/> (accessed July 2025).
- Underwood N. and Powell L. (2019) Challenging the status quo: Innovate or detonate, *Proceedings of FIG Working Week 2019*, Hanoi, Vietnam, 22-26 April, 16pp. ▴

Solar radio bursts impact on the International GNSS Service Network during Solar Cycle 24

This paper has presented an investigation into the effects that solar radio bursts had on the GPS receivers of the International GNSS Service Network during Solar Cycle 24.



Manuel Flores-Soriano
Universidad de Alcalá,
Space Weather
Research Group,
Department of Physics
and Mathematics, Ctra.

Madrid-Barcelona, Km. 33,600, Alcalá
de Henares, 28805, Madrid, Spain

Abstract

Solar radio bursts (SRB) are a known source of noise for Global Navigation Satellite Systems (GNSS) such as GPS or Galileo. They can degrade the carrier-to-noise ratio of satellite signals, thereby diminishing system performance and, in severe cases, causing total service outages. Although a small amount of particularly intense events have already been studied in detail, the commonness and intensity of SRBs that could potentially impair GNSS performance remain uncertain. This study broadens the scope beyond merely extreme SRBs, studying the impact of SRBs on GNSS throughout Solar Cycle 24. Solar 1.4 GHz observations from the Radio Solar Telescope Network are used to find the 20 most intense SRBs at that frequency. The impact of each SRB is then evaluated in terms of GNSS signal strength decrease, reduction in the number of available satellites, and precision degradation. The results show that at the GPS L1 frequency only one event presented extended service degradation, while at the L2 frequency, minimum operational requirements were not met by at least one station during seven of the SRBs. Only a modest correlation between performance degradation and SRB intensity is found. In particular, it is reported how some mild SRBs affected satellite signals while others almost ten times more intense went unnoticed. The fundamental role that the SRB circular polarization plays in these discrepancies is shown with new 1.4 GHz circular polarization observations from the SMOS

satellite. The different responses of GNSS receivers to SRBs depending on the receiver manufacturer are also explored.

1 Introduction

Global navigation satellite systems (GNSS) usually require a minimum carrier-to-noise ratio (C/N_0) of around 30 dBHz for good tracking, or, equivalently, a value of 5 in the standardized 0-to-9 signal strength indicator scale (e.g., IGS/RCTM RINEX WG, 2020). Under normal conditions, satellites at a not-too-low elevation angle over the horizon can easily reach more than 40 dBHz. However, under especial conditions, the C/N_0 can degrade to the point where system performance is affected. This can happen, for example, by variations in the signal power C during ionospheric scintillation triggered during solar flares or geomagnetic storms, or by increasing the amount of background noise N_0 during solar radio bursts (SRB). GNSS systems are, however, polarization sensitive and will only react to the right-hand circularly polarized (RHCP, following the IEEE polarization convention) component of the SRB.

The potential effects of solar radio bursts on GPS were first suggested by Klobuchar et al. (1999). Assuming randomly polarized solar radio bursts, they estimated the amount of flux density required to produce a “just noticeable” 3 dB decrease in GPS signal-to-noise and a potentially more serious 10 dB decrease, finding values of 4×10^4 sfu (solar flux

unit, where $1 \text{ sfu} = 10^{-22} \text{ Wm}^{-2} \text{ Hz}^{-1}$) and $2 \times 10^5 \text{ sfu}$, respectively. Comparing their thresholds with the intensity of historical events they found that only 14 SRBs from the three previous solar activity cycles could have produced a slight decrease in signal-to-noise, and found no SRB able to produce a significant effect on GPS receiver operations.

Chen et al. (2005) reported the first observation of an SRB-induced GPS signal degradation. They found severe signal corruption at dayside International GNSS Service (IGS) stations during the “Halloween” event from 28 October 2003, including a 100% loss of lock during 30 s at one station. By comparing the rate of loss and the solar radio flux at the frequency bands observed by the Radio Solar Telescope Network (RSTN) they found a maximum correlation with the flux at 1.415 GHz, which is located between the GPS L2 signal at 1.228 GHz and L1 at 1.575 GHz. The reported solar flux densities were in the range 4×10^3 to $1.2 \times 10^4 \text{ sfu}$ at that frequency, which is one order of magnitude lower than the proposed threshold in Klobuchar et al. (1999) for a significant impact on GPS. Their study also concludes that the ionospheric perturbations produced by the X-ray and extreme ultraviolet radiation of the flare played only a secondary role.

The 28 October 2003 event was also studied by Cerruti et al. (2006), addressing the sensitivity of GPS systems to SRB polarization with RHCP observations from the Owens Valley Solar Array. They measured a maximum degradation of 3.0 dB at L1 and 10.0 dB at L2. For the event that occurred on 7 September 2005 they measured a C/N_0 decrease of about 2.3 dB and a RHCP flux density of $8 \times 10^3 \text{ sfu}$ for the associated SRB. A theoretical estimation by Cerruti et al. (2006) also found that an SRB with RHCP flux density of 10300 sfu would produce a 3 dB signal fade at L1 and 5.2 dB at L2, for an added semicodeless L2 fade of 8.2 dB.

A series of four intense solar flares took place near solar activity minimum in December 2006, the days 5, 6, 13 and 14.

All but the first presented solar radio bursts associated with GPS signal fades (e.g., Carrano et al., 2009). The most intense event at 1.4 GHz occurred on December 6 with an estimated power of 10^6 sfu RHCP, and lesser values of 6.5×10^5 and $5 \times 10^5 \text{ sfu}$ at 1.2 and 1.6 GHz, respectively (Cerruti et al., 2008). The reported decreases in C/N_0 of 17 dB at L1 and 18–20 dB at L2 were intense enough so that many sunlit IGS receivers did not meet operational requirements as they were tracking fewer than four satellites (Cerruti et al., 2008). Carrano et al. (2009) reported somewhat deeper fades and positioning errors up to 20 m horizontally and 60 m vertically. Clear but milder effects were also reported for the events that occurred on December 13 and 14 (e.g., Cerruti et al., 2008; Afraimovich et al., 2008; Carrano et al., 2009). Interestingly, the event on December 5 did not produce any detectable fade in L1 or L2 signals despite being the most intense of the four December 2006 flares in terms of its X-ray emission (Carrano et al., 2009).

On 24 September 2011, an SRB associated with an M7.1 X-ray flare produced the most intense radio emissions at GNSS frequencies registered during Solar Cycle 24. At 1.4 GHz, the peak intensity of this SRB has been reported to be around $1.1 \times 10^5 \text{ sfu}$ based on observations from the Sagamore Hill RSTN station (e.g., Sreeja et al., 2013, 2014; Muhammad et al., 2015) (however, another RSTN station in San Vito and ESA’s SMOS satellite measured a weaker intensity of around $6 \times 10^4 \text{ sfu}$). Despite being one order of magnitude weaker than the SRB from 6 December 2006, several authors found substantial performance degradation. Sreeja et al. (2013) and Muhammad et al. (2015) reported C/N_0 reductions of around 10 dBHz for GPS L1 and more than 20 dBHz for GPS L2. They also found an increase in position errors and several receivers not meeting minimum operational requirements as they were tracking fewer than four satellites. Sreeja et al. (2014) studied the impact of this same SRB over a real-time precise point positioning service. They found a reduction in the number of tracked satellites and an

increase in the positioning errors from the usual 10–20 cm up to 2.2 m.

Sato et al. (2019) reported a maximum signal strength degradation of 10 dB during the event on 6 September 2017, at a time when the solar flux density was pulsating around $2 \times 10^3 \text{ sfu}$. The authors also detected an increase in positioning error and loss of lock for all GNSS satellites from a possible combined flare and SRB impact.

By means of theoretical analysis, Demyanov et al. (2012) found that solar radio emissions of 10^3 sfu or higher could cause GPS or GLONASS signal tracking failures, especially at the L2 frequency. Huang et al. (2018) conducted a statistical study of GNSS L-band SRBs to evaluate their probability of exceeding a series of five intensity thresholds. Based on 20 years of 1.4 GHz RSTN observations they found 141 SRBs with flux density of at least 10^3 sfu and 21 SRBs with flux density of at least 10^4 sfu . However, as the authors pointed out, RSTN radio flux observations lack polarization information.

The literature reviewed in this introduction shows that the current understanding of how SRBs influence GNSS comes primarily from two types of studies: those that analyze in great detail the most extreme events, and those more theoretical or statistical in nature that, for lack of more concrete observational inputs, have to rely on certain assumptions such as impact thresholds or polarization degrees. This paper aims to help bridge the gap between these two approaches by providing GPS impact statistics that rely on observations rather than on theoretical expectations. By including not only extreme events but also moderate intensity radio bursts, this work can aid in determining intensity thresholds, finding milder events so far overlooked by the community, and better understanding the role that factors such as SRBs polarization or receiver type play on GNSS degradation.

The paper is structured as follows. Section 2 describes the GNSS and solar radio

observations used. Section 3 defines the metrics applied to characterize the GNSS service degradation. Section 4 presents the results, which are discussed in Section 5 in terms of SRB intensity, polarization, frequency dependence and receiver manufacturer. Section 6 summarizes and concludes the paper.

2 Data

2.1 Solar radio observations

The reference solar radio observations used for this work are the 1.4 GHz solar flux density measurements from the RSTN. The RSTN is a global network of solar radio observatories operated by the US Air Force. It has a total of four stations located in Sagamore Hill, USA (station code K7OL); Palehua, USA (PHFF); Learnmonth, Australia (APLM); and San Vito, Italy (LISS). The observations are made available by NOAA at <ftp://ftp.ngdc.noaa.gov/STP/space-weather/solar-data/solar-features/solar-radio/rstn-1-second/>. The frequency of 1.4 GHz was selected for its proximity to the 1.2 GHz of the GPS L2 signal and the 1.6 GHz of the GPS L1 signal.

The events studied in this work are the 20 most intense 1.4 GHz SRBs detected by the RSTN during Solar Cycle 24. The selection of events has been made by automatically searching the highest

fluxes in the available data and manually rejecting false positives such as radio frequency interferences. The peak intensity of the SRB (F_{max}), the instant of maximum intensity ($t_{F_{max}}$), the RSTN stations that observed the SRB and the classification of the associated GOES X-ray flare are shown in Table 1. For SRBs observed by more than one RSTN station, the reported F_{max} value is the average of the maximum intensities measured by each station, while the \pm sign covers the range of F_{max} values observed by all available stations. A larger selection of events is considered unnecessary for the purpose of this work as the weakest selected SRBs already show no large impact on GPS observations.

2.2 GNSS observations

The GNSS performance during SRBs is analyzed using data from the IGS (Johnston et al., 2017). The IGS is a federation of over 200 institutions that provides, among other products, GNSS data from a network of over 500 worldwide stations. Only GPS L1 and L2 signals are used here, as they have the best data availability during Solar Cycle 24. The data were obtained from the Crustal Dynamics Data Information System (CDDIS; Noll, 2010) via <ftp-ssl://gdc.cddis.eosdis.nasa.gov/pub/gps-da-ta/daily>. IGS stations with Sun elevation angles of less than 20 degrees at the time of the peak SRB intensity are not used for this work. Stations with

evident problems unrelated to the SRB, such as data gaps, high levels of noise or a too-low number of tracked satellites in undisturbed conditions, are also discarded.

Certain limitations have to be taken into consideration when comparing 1.4 GHz RSTN observations and GNSS signal degradations from IGS data. The first and most important limitation is the lack of polarimetric information in the RSTN data. GNSS antennas are only sensitive to the RHCP of SRBs, therefore, the RSTN can only provide an upper limit to the RHCP intensity affecting the GNSS receivers. The second limitation is that the 1.4 GHz frequency is not exactly the same as the 1.2 GHz of the GPS L2 signal or the 1.6 GHz of GPS L1. Although the exact implications of this limitation are still not fully known because of the lack of observational input, SRBs can occasionally show sharp transitions in this frequency range (see, e.g., Marqué et al., 2018). Finally, the one-second sampling rate of the RSTN observations is faster than the 30-second rate used here for the GNSS observations. This difference in sampling rates could result in occasional mismatches between the peak SRB intensities and the peak GNSS signal degradation if the burst exhibits a rapid evolution. A resampling of the RSTN observations is discarded because of their frequent clock desynchronizations.

3 Characterization of the GPS degradation

The impact of the 20 selected SRBs on the sunlit IGS GPS stations is characterized here in terms of three parameters: the degradation of the satellite’s signal strength, the reduction in the number of available satellites and the degradation of the satellite’s geometry as measured by the geometric dilution of precision (GDOP). These three parameters are chosen because they are directly accessible from the IGS data (signal strength) or because they are used by final navigation systems users to assess the service integrity (number of available satellites and geometry degradation). More

Table 1. List of the 20 most intense 1.4 GHz SRBs from Solar Cycle 24 observed by the RSTN.

Event ID	F_{max} (10^3 sfu)	$t_{F_{max}}$ (UTC)	RSTN station	GOES flare
01	50.63	15 February 2011, 02:35	APLM	X2.2
02	29.76	7 March 2011, 20:17	K7OL	M3.7
03	86.94 ± 27.21	24 September 2011, 13:05	K7OL, LISS	M7.1
04	3.87 ± 0.13	25 September 2011, 05:41	APLM, LISS	M7.4
05	1.91	23 January 2012, 04:05	APLM	M8.8
06	34.85	4 March 2012, 11:17	LISS	M2.0
07	24.61	5 March 2012, 04:27	PHFF	X1.1
08	5.41	7 March 2012, 01:28	PHFF	X5.4
09	2.56 ± 0.17	17 May 2012, 02:04	APLM, PHFF	M5.1
10	2.08 ± 0.16	14 June 2012, 14:09	K7OL, LISS	M1.9
11	5.46	21 November 2012, 16:12	K7OL	M3.5
12	3.31 ± 0.11	11 April 2013, 06:59	APLM, LISS	M6.5
13	7.53 ± 0.30	4 January 2014, 19:31	K7OL, PHFF	M4.1
14	3.89 ± 0.07	25 February 2014, 00:46	APLM, PHFF	X5.0
15	4.19 ± 0.17	2 April 2014, 13:58	K7OL, LISS	M6.5
16	14.28	25 June 2015, 09:20	APLM	M7.9
17	5.89	4 November 2015, 14:27	K7OL	M3.7
18	19.60	6 September 2017, 12:03	LISS	X9.3
19	3.97	7 September 2017, 10:16	LISS	M7.3
20	8.32	7 September 2017, 14:36	LISS	X1.3

processed parameters, such as position errors, are discarded as they strongly depend on the processing algorithm. Only stations that provide the signal strength in physical units (dBHz) are considered.

The reduction of the satellite’s signal strength is the direct effect of SRBs over the satellite’s signal. In order to isolate the degradation produced by the SRB from other factors affecting the signal strength, such as the elevation angle of the satellite, a quiescent background is used. The quiescent background is obtained by calculating the median signal strength of each satellite using data from three days before and three days after the SRB. The signal fade of each satellite is then calculated by removing the quiescent background from the signal strength during the SRB. The final signal fade is calculated for each IGS station and expressed as the median fade of all observed satellites.

Intense SRBs can cause signal degradation to the point where one or more satellites become unusable. Typically, a minimum of four valid satellites is required for a GNSS receiver to operate. The number of available satellites is therefore an easy and widely used parameter to assess the operational performance of a GNSS system. In practice, satellites with signals weaker than a given threshold are often discarded by GNSS receivers. The exact value of this threshold depends on the particular performance requirements of each user, but for real-time applications, they are typically in the 20–35 dBHz range (e.g., Wang, 2019; Everett et al., 2022). For this work, a threshold of 24 dBHz is used, which corresponds to level 4 in the standardized signal strength indicator scale. The effect of a given SRB on the number of available GPS satellites is classified here according to two categories: moderate, if the signal strength of at least four satellites drops below 24 dBHz relative to the quiescent reference; and severe, if the signal strength of at least seven satellites drops below this 24 dBHz threshold. The final value is expressed as the

percentage of affected IGS stations in each category. The reason to use the decrease in the number of satellites as an indicator, rather than the absolute number of available satellites, is that the latter is highly station-dependent. Even under undisturbed conditions, the number of accessible satellites can vary from 7–8 to about 10–12 depending on the station. The thresholds were selected so that they are meaningful regardless of this variability.

As the SRB reduces the number of available GPS satellites, those that remain tend to be found nearer to the zenith. This leads to a degradation in their geometry that results in larger errors, even

in situations where there are enough available satellites with good signal quality. The multiplicative increase in the error produced by geometric factors is given in terms of the geometric dilution of precision or GDOP (see, e.g., Langley, 1999). In a similar way as for the reduction in the number of available satellites, the effect that SRBs had on the increase of the GDOP is provided here as the percentage of IGS stations that experienced GDOP degradation. Three categories are used: moderate increase, if the GDOP rises by at least five relative to the quiescent reference; severe, if the GDOP increases by at least 20; and a “loss of service” category for the stations

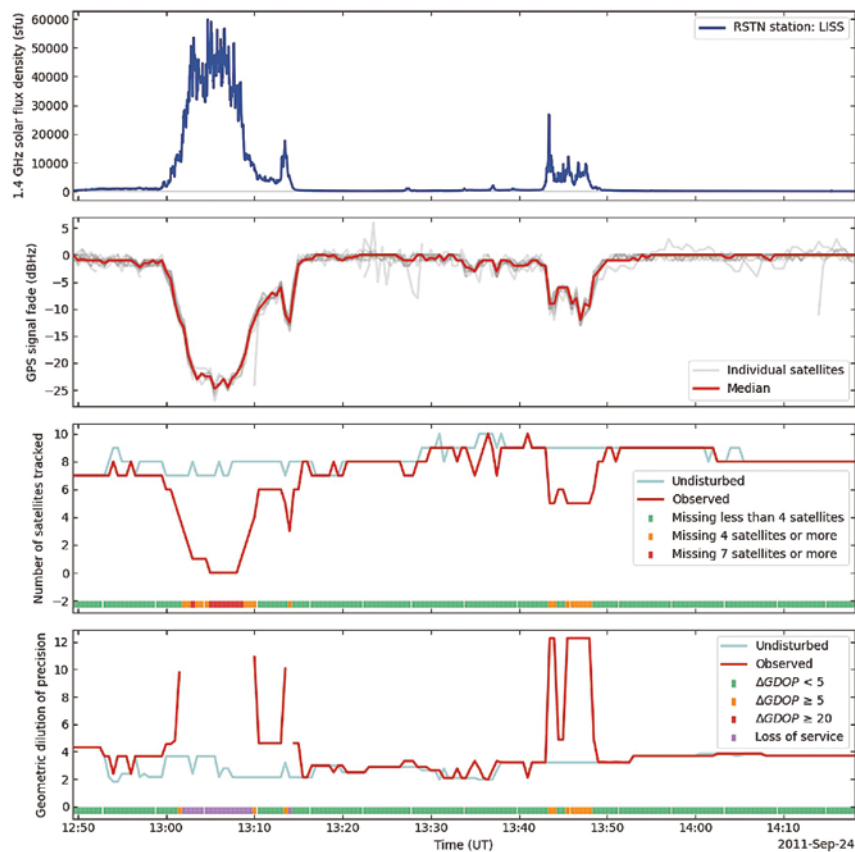


Figure 1. Example of a solar radio burst impacting the GPS service at the L2 frequency. *Top panel:* Solar radio burst on 24 September 2011 observed at 1.4 GHz by the RSTN station LISS. *Second panel from the top:* Signal strength degradation at the IGS station MAS1. The figure is the result of subtracting undisturbed reference observations from the reported signal strength of the satellites during the solar radio burst. *Third panel from the top:* Reduction in the number of available satellites at station MAS1 compared to undisturbed conditions. The severity of the reduction at each instant is color-coded and indicated at the bottom of the panel. The classification in levels of degradation is the same as in Figures 2 and 3, as detailed in the text. A signal strength mask of 24 dBHz is used. *Bottom panel:* Same as the third panel but for the geometric dilution of precision. The gaps indicate a period of time when the system failed to meet minimum operational requirements.

with less than four satellites available. As before, a signal strength mask of 24 dBHz is used. To mitigate the role of eventual overreactions of the GDOP to small changes in the number of satellites, two additional conditions are imposed: first, GDOP degradations produced by the loss of only one satellite are ignored; second, the degradation must have a minimum total duration of at least 150 s.

Figure 1 shows, as an example, the effects that the SRB on 24 September 2011 had on the GPS L2 service frequency at the IGS MAS1 station, in terms of signal strength degradation, reduction in the number of satellites with signals above 24 dBHz and GDOP degradation.

4 Results

Figures 2 and 3 show the impact of the 20 SRBs from Table 1 on the GPS L1 and L2 frequencies, respectively. In both figures, the upper panel illustrates the maximum decrease in signal strength at each IGS station. This is represented using a statistical box plot, where each SRB is depicted by one box. These boxes are arranged in descending order based on the intensity of the SRBs. As in any standard box plot (see, e.g., Smith, 2011), the boxes extend from the lower to the upper quartile, the orange line indicates the median signal fade, and the whiskers enclose the signal fades that fall between these quartiles

and 1.5 times the interquartile distance. Values outside this range are shown as circles and considered statistical outliers in their response to the SRB.

It can be noted from Figure 2 that the signal fades at the GPS L1 frequency were in general mild during Solar Cycle 24. Seven SRBs produced signal fades of at least 5 dBHz, but they affected in most cases just a handful of stations during each event. The only SRB that produced an extended impact in terms of a decrease in the satellite's signal strength was the already wellstudied event on 24 September 2011 (Event 03 in Table 1, see Sect. 1 for references). For it, approximately 75% of IGS stations presented signal fades exceeding 5 dBHz, with a median of 6.6 dBHz and a maximum of 25.7 dBHz. During this event, all seven stations that were equipped with an Allen Osborne Associates (AOA) receiver reported signal fades exceeding 13 dBHz. This occurred despite the Sun elevation angles being relatively low at these stations, ranging from 20 at station ALGO in Canada, to 42 at station SUTM in South Africa. They appear as statistical outliers in the box-plot of this event. The relationship between SRB impact and receiver manufacturer will be addressed in Section 5.

During the SRB on 24 September 2011, twelve out of 74 IGS stations experienced a decrease in the number of available satellites at the L1 frequency by at least four. Three of these stations lost seven satellites and one lost nine. This translated into a total of five stations performing below the minimum operation requirements specified in the previous section. At the GPS L1 frequency, no other event experienced a significant GDOP degradation, despite some of them undergoing a moderate reduction in the number of satellites (bottom and middle panels in Fig. 2, respectively).

As shown in the Introduction, the GPS L2 frequency tends to be more susceptible to SRBs than L1. This effect is also evident by comparing Figures 2 and 3. Seven SRBs were able to degrade the signal strength by at least

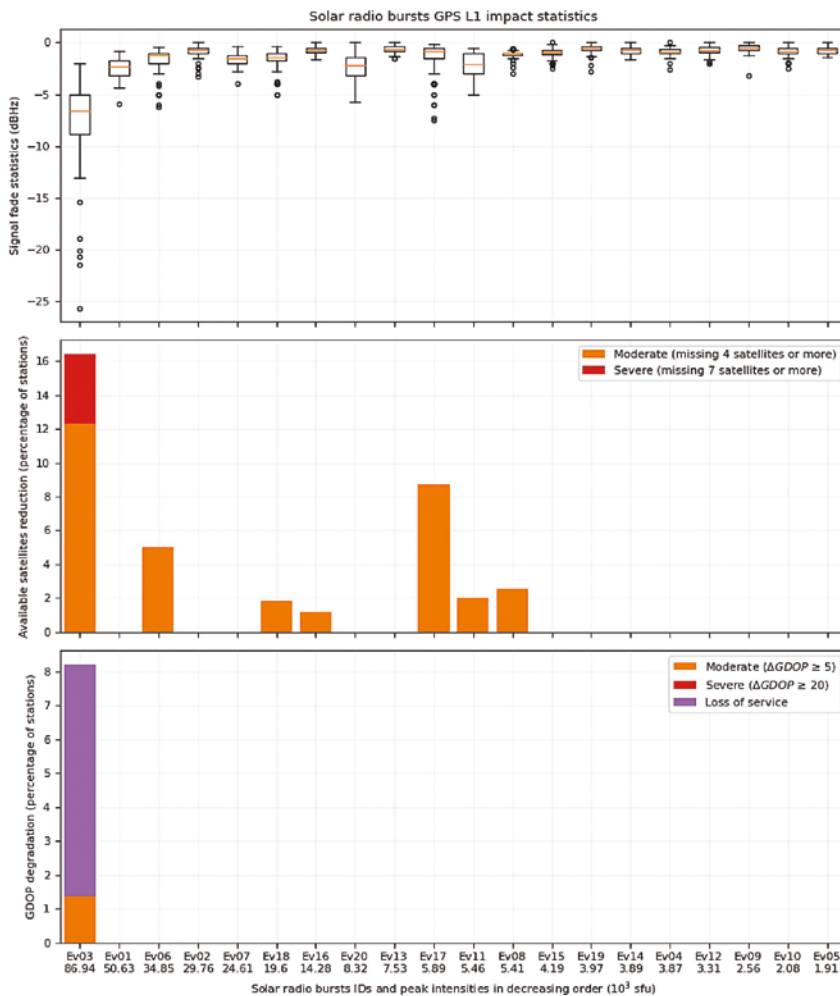


Figure 2. SRB impact statistics at the GPS L1 frequency in terms of signal fading (top panel), reduction in the number of available satellites (middle panel), and GDOP degradation (bottom panel). The signal fade statistics are shown as a box plot for each SRB (see text for details). The reduction in the number of available satellites and the GDOP degradation are presented as stacked bar plots showing the percentage of stations affected at different degradation levels. The SRBs are sorted with decreasing intensity on the x-axis (see Table 1 for SRB details).

5 dBHz at L1. In contrast, ten of them exceeded this threshold at L2, half of which degraded the signal by at least 15 dBHz at one or more stations. The five SRBs that produced signal degradations beyond 15 dBHz are the burston15 February 2011 (Event 01 in Table 1), 24 September 2011, (Event 03), 4 March 2012 (Event 06), 4 November 2015 (Event 17) and 6 September 2017 (Event 18). In the course of these five bursts, a minimum of 10% of the IGS stations experienced a decrease in the number of available satellites by four or more (middle panel in Fig. 3). Specifically, during Events 01 and 06 more than 30% of the stations were affected. The impact was even more significant during Events 17 and 03, with more than 40% and nearly 60% of the stations experiencing this reduction, respectively. The problem was also observed during other SRBs but with only a few stations affected.

At the L2 frequency, seven out of the 20 selected radio bursts resulted in a service degradation that fell below the minimum operational requirements in at least one station (bottom panel in Fig. 3). As for the L1 frequency, the largest effects were observed during the SRB on 24 September 2011 (Event 03). During this event, nearly 40% of the IGS station had less than four satellites with signal strength above 24 dBHz for at least 150 s. Events 01, 06 and 17 produced service degradation at 27%, 17% and 21% of the stations, respectively. For Events 01 and 06 the most common problem was a moderate surge in errors caused by GDOP degradation, with three stations falling short of the minimum operational requirements during each burst. Event 17, on the other hand, had ten stations below minimum operational requirements and four with larger GDOP-related errors.

The GDOP degradation at L2 during Events 18, 11 and 08 was less widespread, impacting only 6–8% of the stations. Although this percentage is lower than during the above-mentioned Events 03, 01, 06 and 17, it is similar to that affecting the L1 frequency during Event 03. Event 08 only produced a moderate error

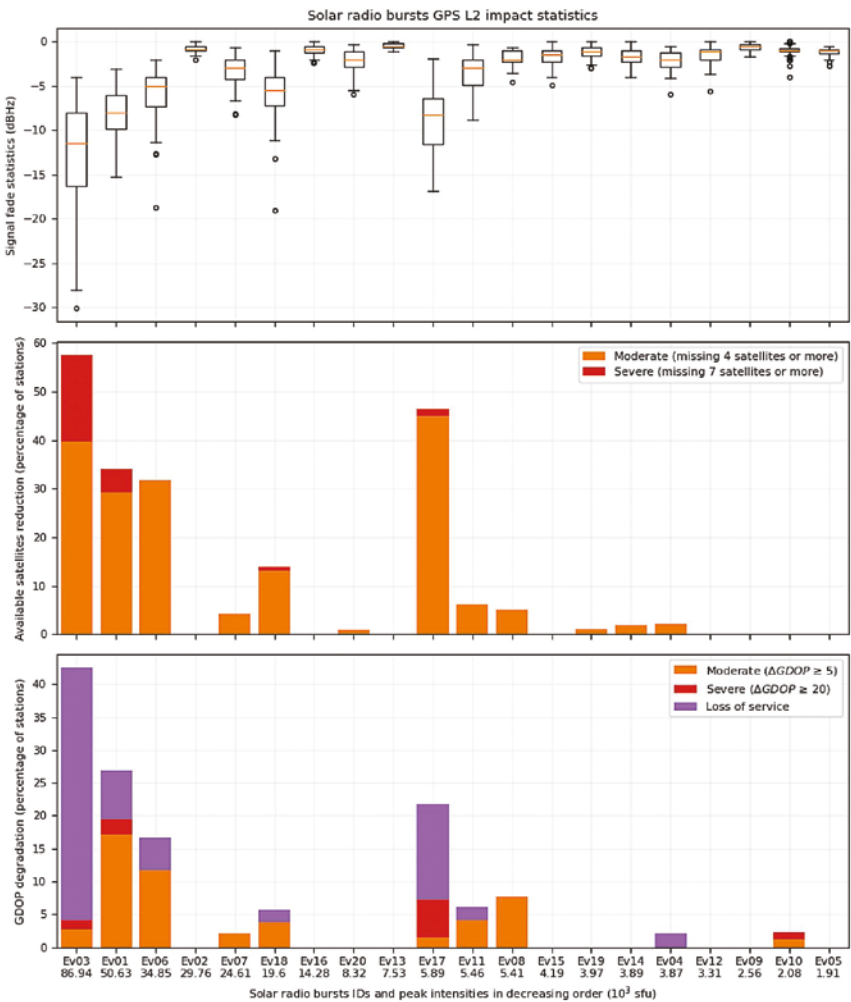


Figure 3. Same as Figure 2 but for the GPS L2 frequency.

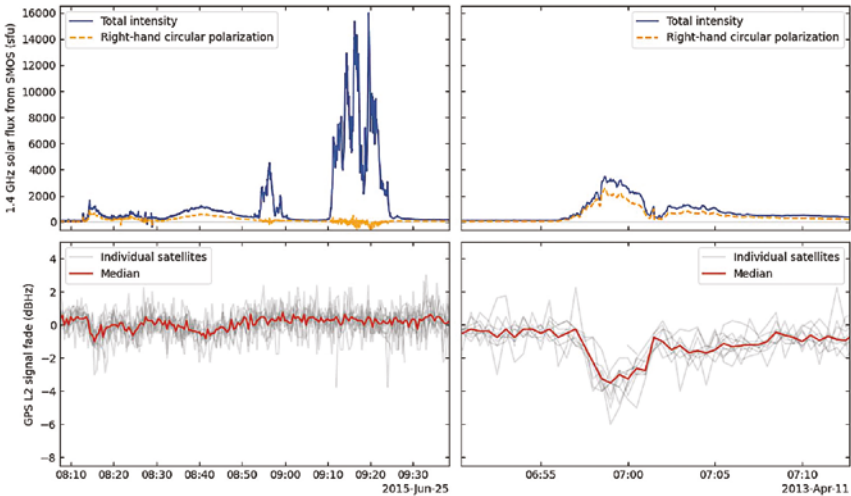


Figure 4. GPS L2 signal fades during the solar radio bursts on 25 June 2015 (left) and on 11 April 2013 (right). It can be noted how the signal fades (bottom panels) correlate well with the right-hand circular polarization of the bursts, but not with their total intensity. The solar radio observations (top panels) are from ESA’s SMOS mission. The GPS L2 data (bottom panels) are from the IGS CHUM station and were recorded with a local solar elevation angle of approximately 55°.

increase, while during Events 18 and 11 two stations each did not meet minimum operational requirements. Despite Event 18 producing somewhat deeper signal fades than Event 11, these two events presented similar service degradation. This is probably because of the short duration of Event 18, which is near the 150 s threshold used for this work. Events 07, 04 and 10 only produced significant service degradation at one or two stations each. These are usually stations that were not operating far from minimum operational requirements in undisturbed conditions.

5 Discussion

5.1 Correlation between GPS signal fades and SRB intensity

Figure 2, and particularly Figure 3, show that the intensity of solar radio bursts and the resulting GPS service degradation do not consistently align. Although it is true that a more intense SRB generally leads to a greater GPS signal disruption, the exceptions to this rule are numerous. For example, Events 02, 16 and 13 went practically unnoticed in the GPS L2 signal despite being the fourth, seventh and ninth most intense bursts, respectively. On the other hand, comparably weaker events, such as Event 17 (tenth most intense), or even Event 12 (17th most intense), resulted in disturbances of

different degrees. Although this modest correlation is not unexpected considering that GNSS receivers only respond to the RHCP of SRBs, it proves that the relation between the total and RHCP intensities is not as direct as often assumed. RHCP observations of SRBs at GNSS frequencies are, however, not as easily available as the total intensity observations used here, which greatly complicates the execution of a similar analysis based on polarization instead of total intensity. The same problem appears when trying to address the limitations of using SRB observations at 1.4 GHz instead of at the 1.575 GHz of L1 or the 1.228 GHz of L2. This subsection discusses the role of polarization and frequency dependencies in the limited correlation between RSTN observations and GPS service degradation.

5.1.1 Polarization dependencies

Two frequent assumptions made in the literature are that SRBs are either fully polarized or totally unpolarized. Figures 2 and 3 suggest that neither of these assumptions is correct. If SRBs were normally unpolarized, then, the RHCP of the bursts would correspond to half the value of their total intensity, making the total intensity a perfectly valid proxy of the RHCP. Conversely, if SRBs were mostly fully polarized, then at least the service degradation produced by the RHCP bursts should show a correlation.

None of these two scenarios is observed in the results from Figures 2 and 3.

Given the shortage of circular polarization observations at GNSS frequencies, the European Space Agency (ESA) has considered the possibility of adding this functionality to its SMOS mission. SMOS is an Earth Explorer satellite originally conceived to perform observations of soil moisture over land and salinity over the oceans using radio interferometry at 1.4 GHz (Mecklenburg et al., 2012). As part of its normal operations, SMOS needs to correct the impact of the Sun in its field of view, which is in fact its strongest source of interference (see, e.g., Camps et al., 2004; Khazâal et al., 2020). The estimated Sun brightness temperature is annotated in the SMOS L1B user product and has been found to show a promising good correspondence with groundbased solar radio observations (Crapolicchio et al., 2018; Flores-Soriano et al., 2021). In view of the potential, but also limitations, of these SMOS data (Flores-Soriano et al., 2021), a new prototype algorithm dedicated specifically to obtaining solar radio observations with SMOS has been developed within the framework of an ESA project. Observations of two solar radio bursts extracted with this prototype algorithm are used here to test the role of the circular polarization in the above-mentioned discrepancies between the SRB total intensity and the depth of the GPS signal fades.

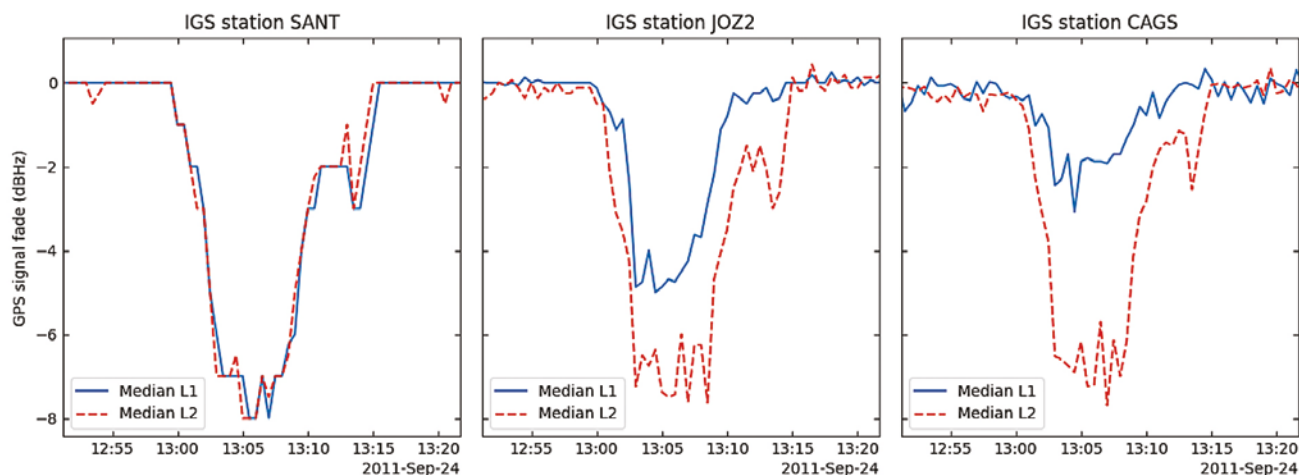


Figure 5. GPS signal fades at the L1 and L2 frequencies measured by three different IGS stations during the main burst of Event 03. To facilitate the comparison, the stations were selected for having similar signal fades at GPS L2. The fades at L1 were, however, different, proving that the relative impact at L1 and L2 does not only depend on the spectral properties of the bursts but also on the station used. From left to right their receivers are Ashtech UZ-12, Leica GRX1200GGPro and Trimble NetR8.

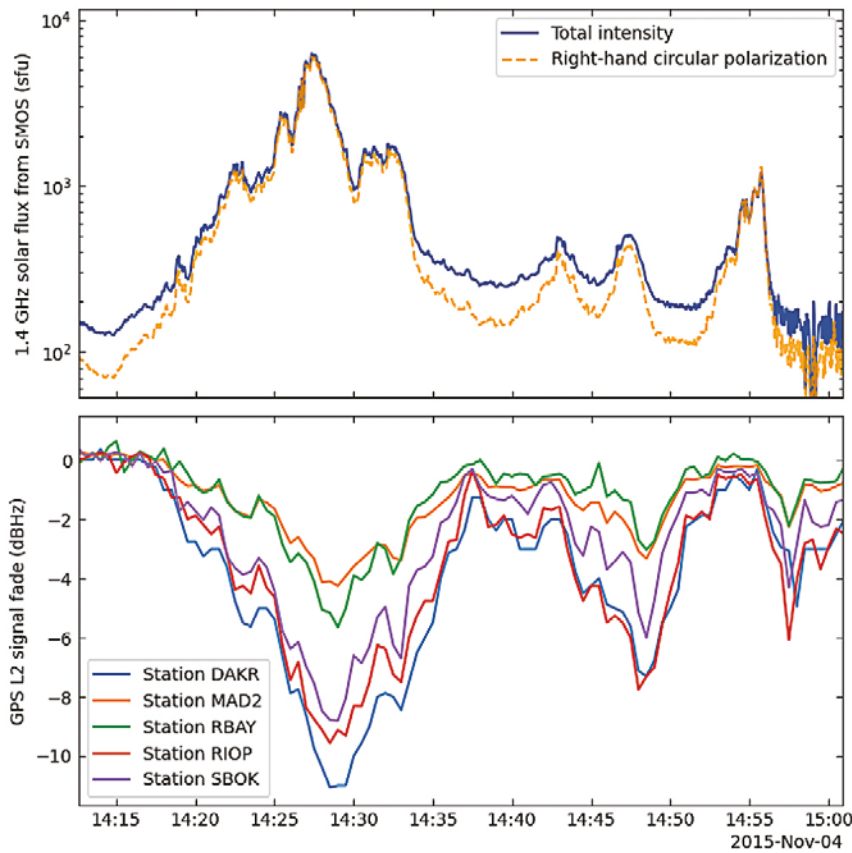


Figure 6. Example of GPS L2 signal fades (bottom panel) whose temporal profile exhibits morphological inconsistencies with the RHCP of the 1.4 GHz SRB (top panel). These inconsistencies are exacerbated by the sharp transition in intensity that the bursts had in the 1.0–1.4 GHz frequency range (see Marqué et al., 2018). The burst corresponds to Event 17 in Table 1. The GPS data are from five random IGS stations and the SRB observations are from SMOS.

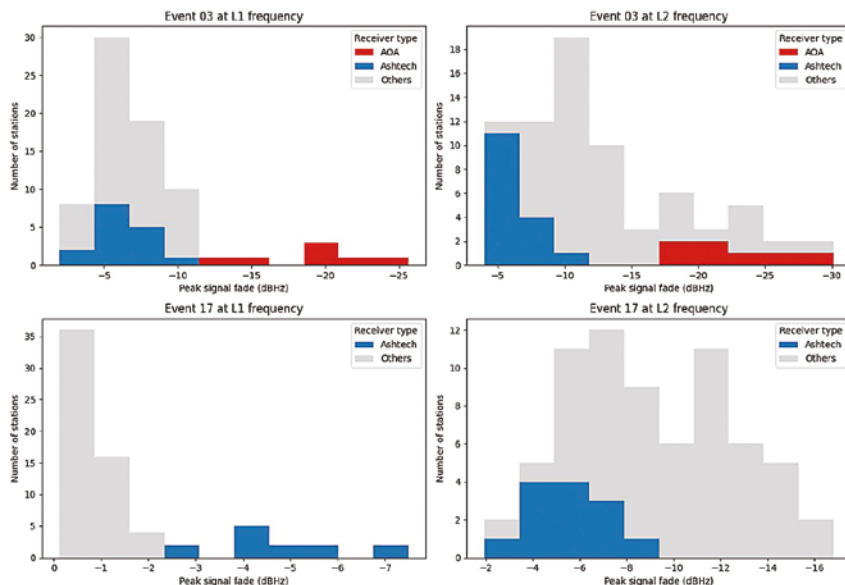


Figure 7. Comparison between the signal fades measured by IGS stations during the SRBs on 24 September 2011 (Event 03 in Table 1, shown in the top panels) and on 4 November 2015 (Event 17, bottom panels), at the L1 and L2 frequencies (left and right panels, respectively), depending on the station's receiver.

The top panels of Figure 4 show the total intensity and circular polarization of the SRBs on 25 June 2015 (Event 16, left in Fig. 4) and on 11 April 2013 (Event 12, right in Fig. 4), as seen by SMOS. These are, respectively, the seventh and 17th most intense of the SRBs selected for this work. The bottom panels show the associated GPS L2 signal fades. To make the GPS signal fades comparable with each other, both were recorded by the same IGS station (CHUM), with a local solar elevation angle close to 55 at the time of peak total radio burst intensity in both cases. The station was equipped with a Trimble NetRS receiver and an AOAD/M_T antenna. The main burst of Event 16 (09:10–09:25) is approximately four times more intense than Event 12. However, the main burst of Event 16 is LHCP, whereas Event 12 has an RHCP of between 70% and 80% of its total intensity. As a result, despite being weaker in terms of total intensity, Event 12 produced a clear decrease in GPS signal strength, unlike the main burst of Event 16. The importance of the circular polarization is also evident when comparing the effects that the different bursts forming Event 16 had on the GPS signal. During Event 16, three minor bursts occurred between 08:10 and 08:50. These bursts were roughly one order of magnitude less intense than the main burst, but in a similar way as Event 12, they were partially RCHP. Once again, the weak RHCP bursts managed to degrade the GPS signal, while the more intense LHCP bursts between 08:50 and 09:25 did not.

Figure 4, while merely an example, clearly demonstrates the limitations of using total intensity observations of SRBs for analyzing GNSS signal degradation. The broad range of polarization states exhibited by these SRBs is such that any attempt to infer RHCP intensities based purely on total intensity observations are bound to be highly uncertain. Establishing a correlation between the depth of GNSS signal fades and the intensity of SRBs requires therefore observations of circular polarization.

5.1.2 Frequency dependence

Addressing the drawbacks of using SRB observations at 1.4 GHz instead of at the GPS L1 and L2 frequencies is hindered by the lack of calibrated solar radio observations at those frequencies. This problem is further exacerbated by the absence of polarization information. One could, in principle, try to correlate the GPS signal fades at L1 and L2 with the SRB intensities at those frequencies (e.g., Sato et al., 2019). Nonetheless, this method is generally incorrect because of differences in how each GPS signal is processed. Furthermore, the processing differs among manufacturers, which could lead to contradictory conclusions depending on the GNSS station used (see also Sect. 5.2). Figure 5 shows, as an example, the differences between the L1 and L2 signal fades at IGS stations SANT, JOZ2 and CAGS during Event 03. Their receivers were, respectively, an Ashtech UZ-12, a Leica GRX1200GGPro and a Trimble NetR8. They were chosen for this example because of their similar signal fades at L2, which facilitates the comparison. The fades at L1 were, however, different by up to almost 6 dBHz, proving that their difference relative to L2 is not simply a matter of different SRB intensities at each GPS frequency.

In terms of morphology, it is not uncommon that GPS signal fades have a close resemblance to their associated 1.4 GHz SRB. Figures 1 and 4 are examples of this. Although this similarity in shape does not provide information about the intensity of the SRB at GPS frequencies, it does suggest that any difference between the SRB at 1.4 GHz and at GPS frequencies was small enough as to maintain the morphology. This is, however, not always the case. Marqué et al. (2018) observed Event 17 across the spectral range from 610 MHz to 1.427 GHz. They reported a peak flux at 1.0 GHz that was 30 times more intense than at 1.4 GHz. If this is interpolated to L2, it results in an approximate difference of a factor of 15 between L2 and 1.4 GHz. The resultant discrepancy

in morphology between the signal fades and the associated 1.4 GHz SRB is shown in Figure 6. This difference in frequency could also partially explain why Event 17 appears somewhat misplaced in Figure 3. If the intensity of Event 17 were tentatively corrected by multiplying it by the aforementioned factor of 15, it would rank as the most or second most intense, which is likely an overestimation based on its impact. This does not apply, however, to Figure 2. There, at the L1 frequency, Event 17 also exhibits anomalously high signal degradation for its comparatively mild intensity at 1.4 GHz.

Yet, according to the data from Marqué et al. (2018), the peak flux of the burst at L1 should have been slightly lower than at 1.4 GHz, not higher. The reason behind this anomaly is probably related to the signal processing, as all affected stations were equipped with an Ashtech receiver (see also the bottom left panel in Figure 7 and the discussion in the next subsection).

A more quantitative strategy for estimating the differences in SRB flux densities between 1.4 GHz, and the GPS L1 and L2 frequencies is by interpolating the polarization observations at 1.0 and 2.0 GHz from the Nobeyama Radio Polarimeters (NoRP). This method has, however, several limitations. SRBs are usually significantly different at these two frequencies, their formation mechanisms and wave modes are not necessarily the same, and the relationship between frequency and flux density is generally non-linear. Six SRBs from Table 1 have NoRP observations available at 1.0 and 2.0 GHz. They are Events 01, 05, 07, 08, 09 and 14. Only data with flux densities above 150 sfu at 1.0 GHz are considered here to avoid comparing background signals. Out of these six radio bursts, one (Event 08) shows a mean difference between the estimated intensities at 1.4 GHz and GPS frequencies of around 5%. Three radio bursts (Events 05, 07, 09) show mean differences of around 15%, while two (Events 01 and 14) show mean differences in the 20–25% range.

5.2 GPS service degradation depending on receiver manufacturer

The statistical outliers in the box plots from Figure 2 suggest that not all GNSS receivers respond to SRBs in the same way. To further explore this dependency, the signal fades at different stations have been compared based on their receiver's manufacturer. Nine different brands have been identified: AOA, Ashtech, JAVAD, JPS, Leica, NovAtel, Septentrio, TPS and Trimble. However, not all brands were present during every event. Figure 7 shows as an example the distribution of the peak signal fades during the SRBs on 24 September 2011 and on 4 November 2015, at the L1 and L2 frequencies. They correspond to Events 03 and 17 in Table 1, respectively. AOA and Ashtech receivers have been highlighted in colour while all the other manufacturers are represented in grey to avoid cluttering. No AOA receiver is depicted for Event 17 as they were not available during this SRB. While AOA and Ashtech were selected for this example because of their clear differences from other receivers, they are not the only brands that display discrepancies (see below).

Figure 7 shows that the response of GNSS receivers to SRBs can vary significantly depending on the manufacturer. During Event 03, AOA receivers exhibited deeper signal fades at the L1 frequency than any of the other available manufacturers. At L2, AOA shows again among the deepest signal fades but with other manufacturers registering similar values. These other stations were, however, more exposed to solar radio noise because of their comparatively higher solar elevation angles (see, e.g., Carrano et al., 2009, for an estimation of the GPS signal fading as a function of the solar incidence angle). During Event 03 Ashtech receivers behaved similarly to other manufacturers at the L1 frequency but showed shallower signal fades at L2. This behaviour of shallower fades at L2 by Ashtech receivers was also observed during Event 17. However, during Event 17 at the L1 frequency, Ashtech receivers showed the deepest signal fades, contrary

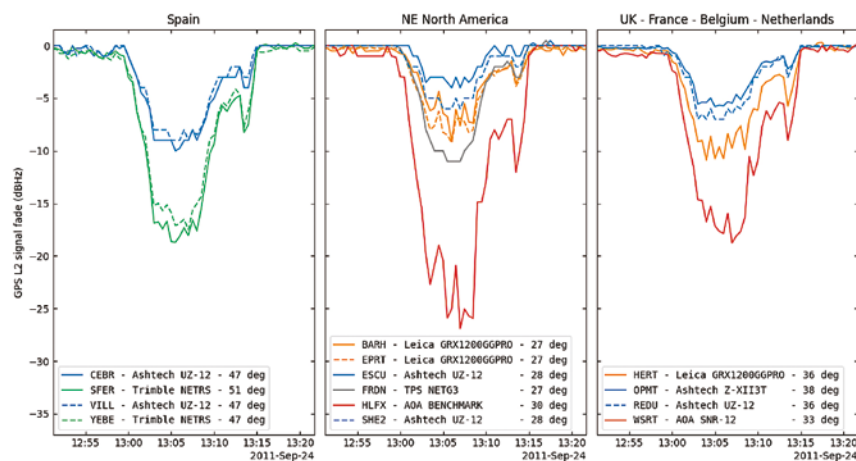


Figure 8. Comparison between the GPS L2 signal fades of GNSS stations situated in the same geographical area depending on their receiver. There are four stations from Spain (left panel), six from the northeast of North America (middle panel) and four stations from the northwest of Europe (right panel). GNSS receivers from the same brand are represented in the same colour. The legend indicates the name of the station, the model of its receiver and the solar elevation angle at the time of maximum SRB emission. It can be noticed how receivers from the same brand tend to behave similarly. The SRB corresponds to Event 03 in Table 1.

to their behaviour during Event 03 at the same frequency. Interestingly, Ashtech receivers displayed similar fades at L1 than at L2 during both events, contrary to the other receivers, which show deeper fades at L2. Another unusual behaviour is displayed by the AOA receivers during the radio burst on 7 March 2011 (not shown here), where the signal fades were deeper at L1 than at L2.

GNSS stations with different equipment, but situated close to each other, offer a good opportunity to compare how they react to SRBs under similar solar elevation angles. Figure 8 shows the fading of the GPS L2 signal during the main burst of Event 03 in three geographical areas: mainland Spain, the northeast of North America (USA and Canada) and the north-west of Europe (United Kingdom, France, Belgium and the Netherlands). In the Spanish group (left panel in Figure 8), there are two stations with an Ashtech receiver and two other stations with a Trimble receiver. The stations with the same type of receiver show similar signal fades, but those from stations with a Trimble receiver are almost 10 dBHz deeper than those from stations with an Ashtech receiver. Similar to the Spanish group, in the groups from the northeast of North America (middle panel) and the northwest of Europe (right panel), the stations with the least deep signal fades are those with an Ashtech receiver. Moreover, in both groups, the station with the deepest signal fades had an AOA receiver (although a different model), while Leica receivers present signal fades intermediate to those of Ashtech and AOA. The repetition of these patterns across different locations permits discarding local factors such as the local noise environment as the primary cause behind these discrepancies.

Even though the differences in their behaviour highlight the importance of considering the specific characteristics of GNSS receivers when assessing the impact of solar radio bursts, a direct comparison between different receivers is not trivial. Their response

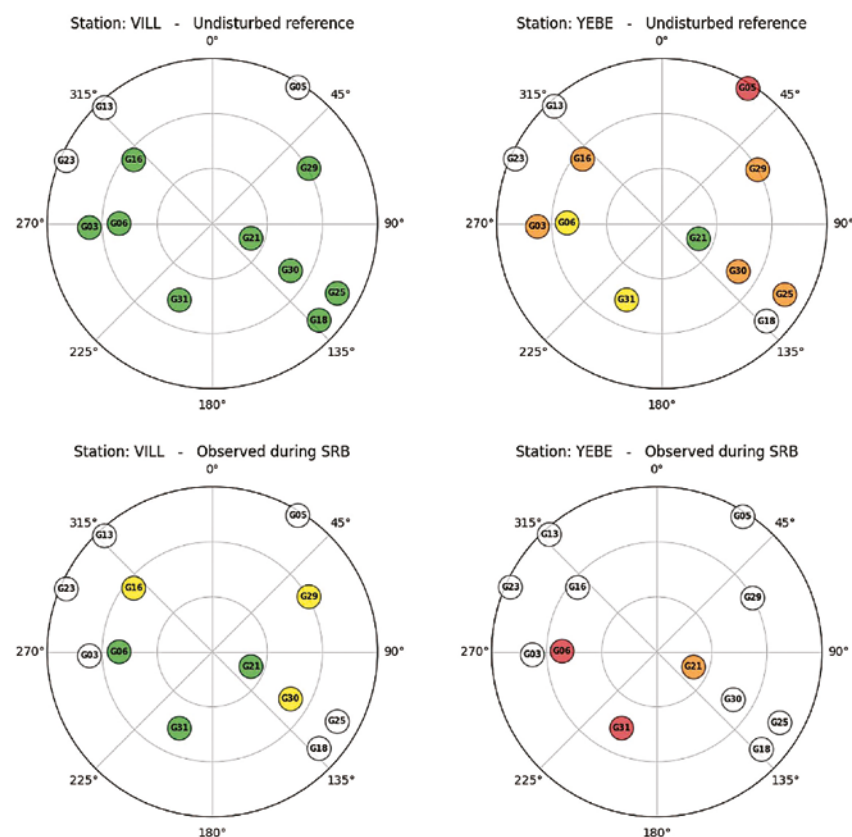


Figure 9. Skyplots with the distribution of GPS satellites and colour-coded L2 signal strength during the SRB on 24 September 2011 at 13:05:30 UTC for IGS stations VILL (left panels) and YEBE (right panels). The colour code is: green (for signal strengths higher than 36 dBHz), yellow (in the range 30–36 dBHz), orange (18–30 dBHz), red (lower than 18 dBHz) and white if the satellite is not available. The thresholds follow the standardized signal strength indicators scale. The top panels indicate the expected undisturbed conditions, while the bottom panels show the conditions observed during the SRB.

to SRBs depends on proprietary or semi-proprietary information and is susceptible to changing through firmware upgrades. Although differences between receivers could make some more resilient against SRB interference than others, it is also plausible that the signal strengths reported by different manufacturers, even though expressed in dBHz units, may not be entirely comparable.

Figures 9 and 10 take a closer look at the comparability between the signal strengths measured by receivers from different manufacturers. The data correspond to stations VILL and YEBE during the SRB on 24 September 2011. These stations are located in central Spain and are separated by an approximate distance of 74 km. YEBE was equipped with a Trimble NetRS receiver and VILL with an Ashtech UZ-12 receiver. The solar elevation angle at the instant of maximum SRB emission was 47°. The top panels of Figure 9 indicate that in normal conditions, both stations should have been tracking nine satellites each, although with significantly higher signal strengths at VILL. Although the signal strength can be conditioned by several factors other than the receiver, a similar scenario is observed at nearby stations CEBR (Ashtech UZ-12 receiver) and SFER (Trimble NetRS). During the SRB (bottom panels in Figure 9), YEBE was tracking at L2 only three satellites, none of them with a signal strength above 20 dBHz. On the other hand, VILL never tracked fewer than six satellites, all of them with signal strengths above 32 dBHz. This indicates that, regardless of signal intensity masks and internal signal strength calculations, YEBE operated during a few minutes below minimum operational conditions, as it was tracking fewer than four satellites in total. VILL, on the other hand, did not encounter this problem. A second difference is that VILL stopped tracking satellites at reported signal strengths significantly higher than YEBE. Figure 10 shows the evolution of the signal strength of four GPS satellites at both stations. It can be noticed how YEBE continued to track satellites until their signal strength fell to approximately

17 dBHz, which is considerably lower than VILL's 32 dBHz. This happens not only during SRB, but also for low-elevation satellites (bottom panels of Fig. 10). These disparities between stations indicate that different receivers may not only respond differently to SRBs, but also that their reported signal strength may not always be directly comparable, not even when they are provided in physical units.

Although the primary focus of the analyses above was on the influence of GNSS receivers on the different responses of GNSS stations to SRBs, GNSS antennas could, in principle, also play a role. Approximately 72% of the receivers used in this study were connected to antennas from the same brand as the receiver. The amount of stations with other receiver antenna combinations is therefore too small to conduct an analysis similar to those performed for the receivers. However, here again, one can examine stations in close proximity to each other, equipped with the same receiver but different antennas, to assess the role of the antenna under otherwise similar conditions. Out of the 12 station pairs used for this test, none of them exhibited a discrepancy in their L2 signal fades persistently exceeding 2 dBHz during SRBs. For example, during the SRB on 24 September 2011 all AOA receivers were connected to AOAD/M_T antennas. Ashtech receivers, on the other hand, were connected to antennas from various manufacturers. IGS stations CEBR and VILL, which are separated by a distance of only 35 km, were both equipped with an Ashtech UZ-12 receiver. The antenna of CEBR was an ASH701945B_M, while the antenna of VILL was an AOAD/M_T (i.e., the same antenna as the AOA receivers.) Despite having different antennas, the behaviour

of CEBR and VILL during the radio burst was practically identical (left panel of Fig. 8), with a maximum difference of just 1 dBHz. Although these tests are far from being an exhaustive analysis of the role of antennas during SRBs, they suggest that receivers have a more significant impact than antennas on the discrepancies observed between stations.

6 Summary and conclusions

This paper has presented an investigation into the effects that solar radio bursts had on the GPS receivers of the International GNSS Service Network during Solar Cycle 24. Focusing on the 20 most intense 1.4 GHz solar radio bursts detected by the RSTN, the impacts were characterized in terms of the degradation of signal strength, reduction in the number of available satellites, and precision decrease as a result of the satellite geometry deterioration.

At the GPS L1 frequency, only the event on 24 September 2011 presents extended service degradation, with 75% of the stations reporting signal fades exceeding 5 dBHz, and five stations operating below minimum operational requirements. At this frequency, the effects of the other radio bursts were noticed only by a few stations and without significant consequences to service integrity.

The impact of solar radio bursts was more pronounced at the GPS L2 frequency. Out of the twenty selected radio bursts, ten caused a reduction in signal strength by at least 5 dBHz at one or more stations. During five of these radio bursts, the degradation exceeded 15 dBHz. Notably, these five radio bursts reduced the number of available satellites by at

The impact of solar radio bursts was more pronounced at the GPS L2 frequency. Out of the twenty selected radio bursts, ten caused a reduction in signal strength by at least 5 dBHz at one or more stations.

least four for between 10% and 60% of the stations. Seven radio bursts produced service degradation below minimum operational requirements, although in three of them, the loss of service was experienced by only one or two stations. To the best of this author's knowledge, the impact on GNSS during several of these events, such as Events 01, 06, 08, 11 and 17, has yet not been studied in detail elsewhere. Particularly in the current situation of insufficient SRB observations with polarization at GPS frequencies, having a diverse set of events is crucial for determining an empirical relationship between burst intensity and GPS service degradation.

Although the degradations of GPS signals shown in this paper are a consequence of the noise introduced by solar radio bursts, their correlation with the burst intensities is found to be modest at best. This can be at least partially explained by the fact

that GPS systems are sensitive only to the right-hand circular polarization of the burst and that the available observations of solar radio bursts lack polarization information. Experimental solar radio observations from the SMOS mission, which include polarization data, show enhanced correlation and a diversity of polarization states that underscores the importance of incorporating polarization when examining the relationship between radio bursts and the disturbances they cause in polarization-sensitive systems such as GNSS. Given these findings, trying to establish solar radio burst intensity thresholds that could be of use to affected GNSS users is only feasible when polarization information is available. Adding to SMOS the capability to provide solar radio observations could help address this issue. Having been in orbit since 2010, SMOS could provide a large enough dataset of SRB observations to help establish intensity thresholds, while also aiding in understanding how

subsequent GNSS service upgrades have improved the resilience of GNSS systems against SRBs. Furthermore, adding these solar radio observations as one of the near real-time SMOS products would provide affected users with a monitoring service.

The drawbacks of using SRB observations at 1.4 GHz instead of at GPS frequencies have also been addressed. At least one SRB (Event 17) displays significant discrepancies in both intensity and shape. A tentative analysis using NoRP polarization observations at 1.0 GHz and 2.0 GHz suggests that discrepancies of up to 20–25% between the SRB intensities at GPS frequencies and at 1.4 GHz are probably not uncommon.

This paper has also explored how different receivers respond to the same radio burst. It was observed that receivers from different manufacturers may exhibit different degrees of impact, even when other factors such as the solar elevation angle are held approximately the same. The signal strength of the satellites during the radio bursts was found to be manufacturer-dependent, even when the stations provided the measurement in units of dBHz. A variation in receiver response was also noticed in the relative depths of the signal fades at L1 and L2. These dependencies complicate the task of establishing intensity thresholds, as the impact is receiver-specific. It is however worth noting that the current situation may differ somewhat from the conditions during Solar Cycle 24, from which the GPS data used in this study were obtained. Since then, some manufacturers have been acquired by other companies, new stations have been added to the IGS Network, and others have been upgraded.

At this point it is probably pertinent to issue some words of caution. Solar flares and solar radio bursts are distinct phenomena and have different impacts on GNSS systems. This fact is well known within the scientific community but it is too often overlooked by final users of space weather services. Users of radio systems affected by space weather conditions often rely on impact scales

The drawbacks of using SRB observations at 1.4 GHz instead of at GPS frequencies have also been addressed. At least one SRB (Event 17) displays significant discrepancies in both intensity and shape.

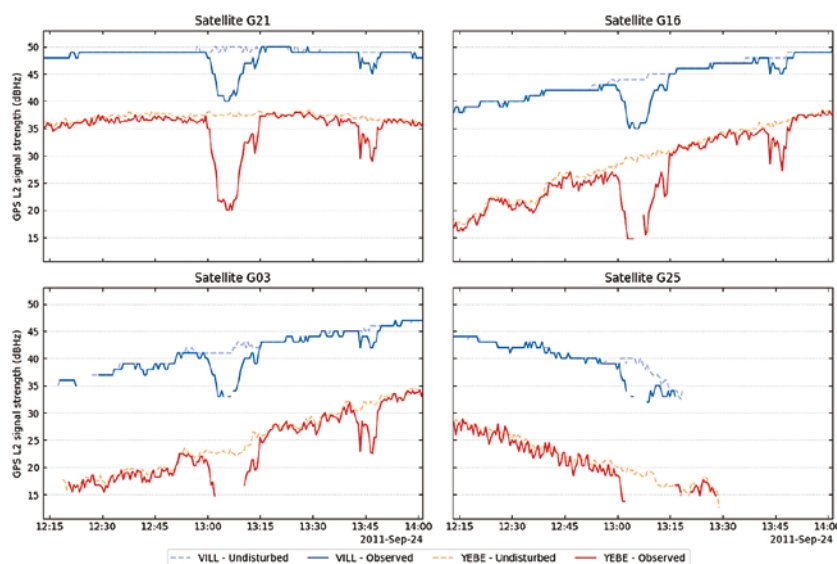


Figure 10. GPS L2 signal strengths of four GPS satellites as measured at IGS station VILL (blue) and YEBE (red) during the SRB on 24 September 2011 (solid line) and according to the undisturbed reference (dashed line). The stations are separated by an approximate distance of 74 km. Their receivers are an Ashtech UZ-12 (VILL) and a Trimble NetRS (YEBE).

that use the intensity of solar flares as a threshold, such as NOAA's scale for radio blackouts. These scales are, however, not applicable to disturbances caused by solar radio bursts, as the intensities of flares and radio bursts do not correlate. The results of this paper are a good example of this. Among the four events with the largest impact on GPS, only Event 01 was an X-class flare, while the other three were relatively mild flares with intensities between M2.0 and M7.1 (see Table 1). On the other hand, out of the six X-class flares, only two (Events 01 and 18) had an impact on GPS. This absence of impact during intense flares also suggests that, at least for the metrics and GNSS sampling rates used in this study, the ionospheric perturbations produced by flares have a negligible influence on GNSS impact compared to SRBs.

Acknowledgements

This work was supported by the ESA contract “Synergic use of SMOS L1 Data in Sun Flare Detection and Analysis” and project PID2020-119407GB-I00/AEI/10.13039/50110 0011033. The author is very thankful to the participants of the “Synergic use of SMOS L1 Data in Sun Flare Detection and Analysis” ESA project for their effort in generating the SMOS solar observations and for the fruitful discussions. The RSTN is operated by the US Air Force and the observations made available by NOAA at <ftp://ftp.ngdc.noaa.gov/STP/space-weather/solar-data/solar-features/solar-radio/rstn-1-second/>. The data from the IGS Network (Johnston et al., 2017) were obtained from the Crustal Dynamics Data Information System (CDDIS; Noll, 2010) via <ftp://gdc.cddis.eosdis.nasa.gov/pub/gps/data/daily>. The Nobeyama Radio Polarimeters (NoRP) are operated by Solar Science Observatory, a branch of the National Astronomical Observatory of Japan, and their observing data are verified scientifically by the consortium for NoRP scientific operations. Their data are available at <https://solar.nro.nao.ac.jp/norp/html/daily/>. The research presented in this paper has made use of the following Python libraries:

(Astropy Collaboration et al., 2013, 2018, 2022), Georinex (Hirsch et al., 2019), Matplotlib (Hunter, 2007), NumPy (Harris et al., 2020) and Pandas (McKinney, 2010; Reback et al., 2022). The editor thanks two anonymous reviewers for their assistance in evaluating this paper.

References


- Afraimovich E, Demyanov V, Ishin A, Smolkov G. 2008. Powerful solar radio bursts as a global and free tool for testing satellite broadband radio systems, including GPS-GLONAS-GALILEO. *J Atmos Sol-Terr Phys* **70(15)**: 1985–1994. <https://doi.org/10.1016/j.jastp.2008.09.008>.
- Astropy Collaboration, Price-Whelan AM, Lim PL, Earl N, Starkman N, et al. 2022. The Astropy project: sustaining and growing a community-oriented open-source project and the Latest Major Release (v5.0) of the Core Package. *Astrophys J* **935(2)**: 167. <https://doi.org/10.3847/1538-4357/ac7c74>.
- Astropy Collaboration, Price-Whelan AM, Sipőcz BM, Günther HM, Lim PL, et al. 2018. The Astropy Project: building an open-science project and status of the v2.0 Core Package. *Astron J* **156(3)**: 123. <https://doi.org/10.3847/1538-3881/aabc4f>.
- Astropy Collaboration, Robitaille TP, Tollerud EJ, Greenfield P, Droettboom M, et al. 2013. Astropy: a community Python package for astronomy. *A&A* **558**: A33. <https://doi.org/10.1051/0004-6361/201322068>.
- Camps A, Vallosera M, Duffo N, Zapata M, Corbella I, Torres F, Barrera V. 2004. Sun effects in 2-D aperture synthesis radiometry imaging and their cancelation. *IEEE Trans Geosci Remote Sens* **42(6)**: 1161–1167.
- Carrano CS, Bridgwood CT, Groves KM. 2009. Impacts of the December 2006 solar radio bursts on the performance of GPS. *Radio Sci* **44(1)**: RS0A25. <https://doi.org/10.1029/2008RS004071>.
- Cerruti AP, Kintner PM, Gary DE, Lanzerotti LJ, de Paula ER, Vo HB. 2006. Observed solar radio burst effects on GPS/wide area augmentation system carrier-to-noise ratio. *Space Weather* **4(10)**: S10006. <https://doi.org/10.1029/2006SW000254>.
- Cerruti AP, Kintner Jr. PM, Gary DE, Mannucci AJ, Meyer RF, Doherty P, Coster AJ. 2008. Effect of intense December 2006 solar radio bursts on GPS receivers. *Space Weather* **6(10)**: S10D07. <https://doi.org/10.1029/2007SW000375>.
- Chen Z, Gao Y, Liu Z. 2005. Evaluation of solar radio bursts' effect on GPS receiver signal tracking within International GPS Service network. *Radio Sci* **40(3)**: RS3012. <https://doi.org/10.1029/2004RS003066>.
- Crapolicchio R, Casella D, Marqué C. 2018. Solar radio observations from Soil Moisture and Ocean Salinity (SMOS) mission. In: IGARSS 2018 2018 IEEE International Geoscience and Remote Sensing Symposium, Valencia, Spain, 22–27 July, IEEE, pp. 4111–4114. <https://doi.org/10.1109/IGARSS.2018.8518756>.
- Demyanov VV, Afraimovich EL, Jin S. 2012. An evaluation of potential solar radio emission power threat on GPS and GLONASS performance. *GPS Solut* **16(4)**: 411–424. <https://doi.org/10.1007/s10291-011-0241-9>.
- Everett T, Taylor T, Lee D-K, Akos DM. 2022. Optimizing the use of RTKLIB for smartphone-based GNSS measurements. *Sensors* **22(10)**: 3825. <https://doi.org/10.3390/s22103825>.
- Flores-Soriano M, Cid C, Crapolicchio R. 2021. Validation of the

- SMOS mission for space weather operations: the potential of near real-time solar observation at 1.4 GHz. *Space Weather* **19**(3): e2020SW002649. <https://doi.org/10.1029/2020SW002649>.
- Harris CR, Millman KJ, van der Walt SJ, Gommers R, Virtanen P, et al. 2020. Array programming with NumPy. *Nature* **585**(7825): 357–362. <https://doi.org/10.1038/s41586-020-2649-2>.
- Hirsch M, Mayorov N, Strandberg J. 2019. Scivision/georinex: File extension agnostic. *Zenodo*. <https://doi.org/10.5281/zenodo.2580306>.
- Huang W, Aa E, Shen H, Liu S. 2018. Statistical study of GNSS L-band solar radio bursts. *GPS Solut* **22**(4): 114. <https://doi.org/10.1007/s10291-018-0780-4>.
- Hunter JD. 2007. Matplotlib: a 2D graphics environment. *Comput Sci Eng* **9**(3):90–95. <https://doi.org/10.1109/MCSE.2007.55>.
- IGS/RCTM RINEX WG. 2020. RINEX – The receiver independent exchange format (Version 3.05). Available at <https://files.igs.org/pub/data/format/rinex305.pdf>.
- Johnston G, Riddell A, Hausler G. 2017. The International GNSS Service. In: *Springer handbook of global navigation satellite systems*, Teunissen PJ, Montenbruck O (Eds.), Springer, Cham, pp. 967–982, ISBN 978-3-319-42928-1. <https://doi.org/10.1007/978-3-319-42928-1>.
- Khazâal A, Cabot F, Anterrieu E, Kerr YH. 2020. A new direct Sun correction algorithm for the soil moisture and ocean salinity space mission. *IEEE J Sel Top Appl Earth Obs Remote Sens* **13**: 1164–1173. <https://doi.org/10.1109/JSTARS.2020.2971063>.
- Klobuchar JA, Kunches JM, VanDierendonck AJ. 1999. Eye on the Ionosphere: potential solar radio burst effects on GPS signal to noise. *GPS Solut* **3**(2):6–971. <https://doi.org/10.1007/PL00012794>.
- Langley RB. 1999. Dilution of precision. *GPS World* **10**(5):52–59.
- Marqué C, Klein K-L, Monstein C, Opgenoorth H, Pulkkinen A, Buchert S, Krucker S, Van Hoof R, Thulesen P. 2018. Solar radio emission as a disturbance of aeronautical radionavigation. *J Space Weather Space Clim* **8**:A42. <https://doi.org/10.1051/swsc/2018029>.
- McKinney W. 2010. Data structures for statistical computing in python. In: *Proceedings of the 9th Python in Science Conference*, Van der Walt S, Millman J (Eds), SciPy, Austin, Texas, pp. 56–61.
- Mecklenburg S, Drusch M, Kerr Y, Font J, Martín-Neira M, et al. 2012. ESA's soil moisture and ocean salinity mission: mission performance and operations. *IEEE Trans Geosci Remote Sens* **50** (5): 1354–1366. <https://doi.org/10.1109/TGRS.2012.2187666>.
- Muhammad B, Alberti V, Marassi A, Cianca E, Messerotti M. 2015. Performance assessment of GPS receivers during the September 24, 2011 solar radio burst event. *J Space Weather Space Clim* **5**: A32. <https://doi.org/10.1051/swsc/2015034>.
- Noll CE. 2010. The crustal dynamics data information system: A resource to support scientific analysis using space geodesy. *Adv Space Res* **45**(12): 1421–1440. <https://doi.org/10.1016/j.asr.2010.01.018>.
- Reback J, Jbrockmendel, McKinney W, den Bossche JV, Augspurger T, et al. 2022. pandasdev/pandas: Pandas 1.4.2, *Zenodo*. <https://doi.org/10.5281/zenodo.6408044>.
- Sato H, Jakowski N, Berdermann J, Jiricka K, Heselbarth A, Banyś D, Wilken V. 2019. Solar radio burst events on 6 September 2017 and its impact on GNSS signal frequencies. *Space Weather* **17**(6): 816–826. <https://doi.org/10.1029/2019SW002198>.
- Smith G. 2011. *Descriptive statistics, Chapter 3*, 1st edn., Academic Press.
- Sreeja V, Aquino M, de Jong K. 2013. Impact of the 24 September 2011 solar radio burst on the performance of GNSS receivers. *Space Weather* **11**(5):306–312. <https://doi.org/10.1002/swe.20057>.
- Sreeja V, Aquino M, de Jong K, Visser H. 2014. Effect of the 24 September 2011 solar radio burst on precise point positioning service. *Space Weather* **12**(3): 143–147. <https://doi.org/10.1002/2013SW001011>.
- Wang Y. 2019. Localization precise in urban area. *Theses*. Institut National Polytechnique de Toulouse – INPT, Available at https://theses.hal.science/tel-02917137v2/file/Wang_-_Yu.pdf.

Cite this article as: Flores-Soriano M. 2024. Solar radio bursts impact on the International GNSS Service Network during Solar Cycle 24. *J. Space Weather Space Clim*. 14, 32. <https://doi.org/10.1051/swsc/2024034>.

© M. Flores-Soriano, originally published by EDP Sciences 2024.

This is an Open Access article distributed under the terms of the Creative Commons Attribution License (<https://creativecommons.org/licenses/by/4.0>), which permits unrestricted use, distribution, and reproduction in any medium, provided the original work is properly cited.

The article is republished with the author's permission. 

GNSS Constellation

Specific Monthly Analysis

Summary: July 2025

The analysis performed in this report is solely his work and own opinion. State Program: U.S.A (G); EU (E); China (C) "Only MEO- SECM satellites"; Russia (R); Japan (J); India (I)



Narayan Dhital
Actively involved to support international collaboration in GNSS-related activities. He has regularly supported and contributed to different workshops of the International Committee on GNSS (ICG), and the United Nations Office for Outer Space Affairs (UNOOSA). As a professional employee, the author is working as GNSS expert at the Galileo Control Center, DLR GfR mbH, Germany.

Introduction

This article continues the monthly performance analysis of the GNSS constellation. Readers are encouraged to refer to previous issues for foundational discussions and earlier results.

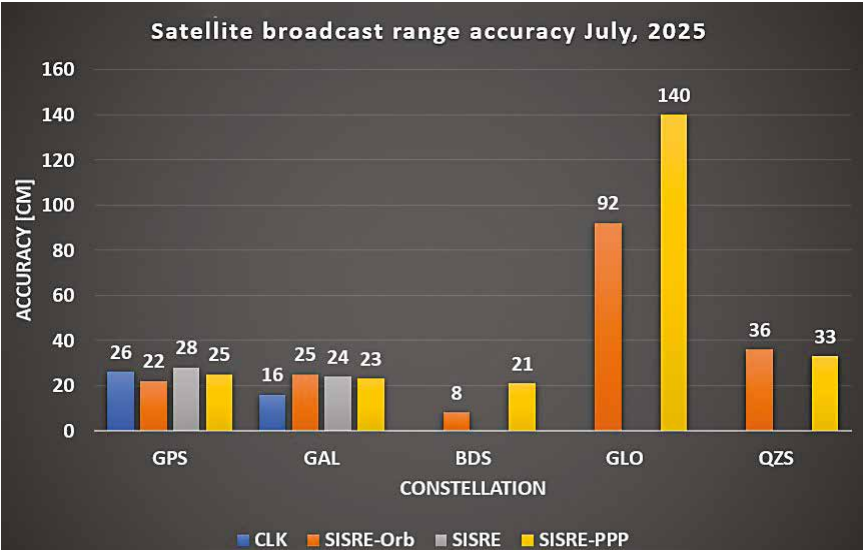
Analyzed Parameters for July 2025

(Dhital et. al, 2024) provides a brief overview of the necessity and applicability of monitoring the satellite clock and orbit parameters.

a. Satellite Broadcast Accuracy, measured in terms of **Signal-In-Space Range Error (SISRE)** (Montenbruck et. al, 2010).

- b. **SISRE-Orbit** (only orbit impact on the range error), SISRE (both orbit and clock impact), and **SISRE-PPP** (as seen by the users of carrier phase signals, where the ambiguities absorb the unmodelled biases related to satellite clock and orbit estimations. Satellite specific clock bias is removed) (Hauschlid et.al, 2020)
- c. **Clock Discontinuity:** The jump in the satellite clock offset between two consecutive batches of data uploads from the ground mission segment. It is indicative of the quality of the satellite atomic clock and associated clock model.
- d. **URA:** User Range Accuracy as an indicator of the confidence on the accuracy of satellite ephemeris. It is mostly used in the integrity computation of RAIM.
- e. **GNSS-UTC offset:** It shows stability of the timekeeping of each constellation w.r.t the UTC

(a), (b) Satellite Clock and Orbit Accuracy (monthly RMS values)



Note:- for India’s IRNSS there are no precise satellite clocks and orbits as they broadcast only 1 frequency which does not allow the dual frequency combination required in precise clock and orbit estimation; as such, only URA and Clock Discontinuity is analyzed.

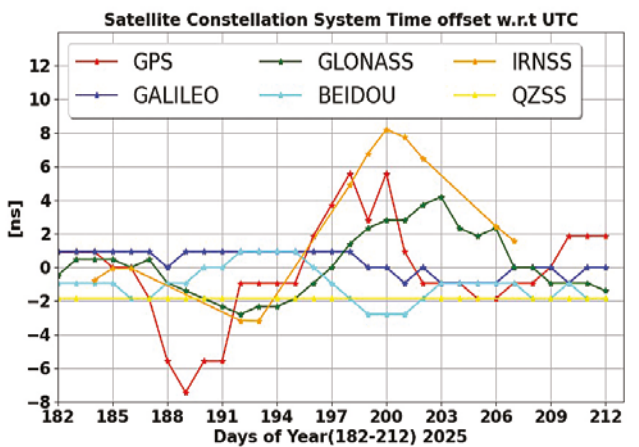
(c) Satellite Clock Jump per Mission Segment Upload

Const	Mean [ns]	Max [ns]	95_ Percentile [ns]	99_ Percentile [ns]	Remark (Best and Worst 95 %)
IRNSS	2.41	173.30	4.13	14.30	Best I02 (3.18 ns) Worst I10 (8.83 ns) Big jumps for each satellite in multiple days.
GPS	0.37	7.96	0.73	2.21	Best G15 (0.40 ns) Worst G03 (2.88 ns) G02 and G14, both, had jump upto 8 ns on the 25th and 31st July, respectively.
GAL	47.76	2278049.15	0.18	0.43	Best E02 (0.13 ns) Worst E19 (0.36 ns). There was a large clock jump for E30 on the 18th July.

(d) User Range Accuracy (Number of Occurrences in Broadcast Data 01–31 July)

IRNSS-SAT	2 [m]	2.8 [m]	4.0 [m]	5.7 [m]	8 [m]	8192 [m]	9999.9 [m]	Remark Other URA values (frequency)
I02	2954	53	2	-	1	-	-	-
I06	3012	-	-	-	1	-	-	-
I09	536	2	-	-	1	-	-	-
I10	500	-	-	-	-	-	-	-

(e) GNSS-UTC Offset



Monthly Performance Remarks:

- 1. Satellite Clock and Orbit Accuracy:
 - The performance of all constellations remained like last months. No significant observations to be reported.

- The URA and satellite clock discontinuity for IRNSS showed some improvement. The URA values are less scattered (as was the case in last month as well).
- 2. UTC Prediction (GNSS-UTC):
 - GPS provided the most deviation in its prediction. All other constellations reported relatively stable and consistent (to last months) UTC predictions.

References

Alonso M, Sanz J, Juan J, Garcia, A, Casado G (2020) Galileo Broadcast Ephemeris and Clock Errors Analysis: 1 January 2017 to 31 July 2020, MDPI

Alonso M (2022) Galileo Broadcast Ephemeris and Clock Errors, and Observed Fault Probabilities for ARAIM, Ph.D Thesis, UPC

Bento, M (2013) Development and Validation of an IMU/GPS/Galileo Integration Navigation System for UAV, PhD Thesis, UniBW.

BIMP (2024 a) https://e-learning.bipm.org/pluginfile.php/6722/mod_label/intro/User_manual_cggtts_analyser.pdf?time=1709905608656

BIMP (2024 b) <https://e-learning.bipm.org/mod/folder/view.php?id=1156&forceview=1>

BIMP (2024 c) <https://cggtts-analyser.streamlit.app>

Bruggemann, Troy & Greer, Duncan & Walker, R.. (2011). GPS fault detection with IMU and aircraft dynamics. IEEE Transactions on Aerospace and Electronic Systems - IEEE TRANS AEROSP ELECTRON SY. 47. 305-316. 10.1109/TAES.2011.5705677.

Cao X, Zhang S, Kuang K, Liu T (2018) The impact of eclipsing GNSS satellites on the precise point positioning, Remote Sensing 10(1):94

Chen, K., Chang, G. & Chen, C (2021) GINav: a MATLAB-based software for the data processing and analysis of a GNSS/IMU integrated navigation system. GPS Solut 25, 108. <https://doi.org/10.1007/s10291-021-01144-9>

Curran, James T. & Broumendan, Ali. (2017). On the use of Low-Cost IMUs for GNSS Spoofing Detection in Vehicular Applications.

Dhital N (2024a) GNSS constellation specific monthly analysis summary, Coordinates, Vol XX, Issue 1, 2, 3, 4

- Dhital N (2024b) GNSS constellation specific monthly analysis summary, Coordinates, Vol XX, Issue 6, 7
- Dhital N (2025) GNSS constellation specific monthly analysis summary, Coordinates, Vol XXI, Issue 1
- GINAv (2025). <https://geodesy.noaa.gov/gps-toolbox/GINav.shtml>
- Goercke, L (2017) GNSS-denied navigation of fixed-wing aircraft using low-cost sensors and aerodynamic motion models, PhD Thesis, TUM.
- GROOPS (2025) GROOPS Documentation and Cookbook. <https://groops-devs.github.io/groops/html/index.html>
- Guo, Jing & Chen, Guo & Zhao, Qile & Liu, Jingnan & Liu, Xianglin. (2017). Comparison of solar radiation pressure models for BDS IGSO and MEO satellites with emphasis on improving orbit quality. GPS Solutions. 21. 10.1007/s10291-016-0540-2.
- Guo F, Zhang X, Wang J (2015) Timing group delay and differential code bias corrections for BeiDou positioning, J Geod,
- Hauschlid A, Montenbruck O (2020) Precise real-time navigation of LEO satellites using GNSS broadcast ephemerides, ION
- IERS C04 (2024) <https://hpiers.obspm.fr/iers/eop/eopc04/eopc04.1962-now>
- IGS (2019) GNSS Attitude Quaternions Exchange using ORBEX
- IGS (2021) RINEX Version 4.00 https://files.igs.org/pub/data/format/rinex_4.00.pdf
- InsideGNSS (2024) Working papers: upgrading galileo <https://insidegnss.com/working-papers-upgrading-galileo/>
- Jiabo G, Xingyu Z, Yan C, Mingyuan Z (2021) Precision Analysis on Reduced-Dynamic Orbit Determination of GRACE-FO Satellite with Ambiguity Resolution, Journal of Geodesy and Geodynamics (<http://www.jgg09.com/EN/Y2021/V41/I11/1127>)
- Kj, Nirmal & Sreejith, A. & Mathew, Joice & Sarpotdar, Mayuresh & Suresh, Ambily & Prakash, Ajin & Safonova, Margarita & Murthy, Jayant. (2016). Noise modeling and analysis of an IMU-based attitude sensor: improvement of performance by filtering and sensor fusion. 99126W. 10.1117/12.2234255.
- Li M, Wang Y, Li W (2023) performance evaluation of real-time orbit determination for LUTAN-01B satellite using broadcast earth orientation parameters and multi-GNSS combination, GPS Solutions, Vol 28, article number 52
- Li W, Chen G (2023) Evaluation of GPS and BDS-3 broadcast earth rotation parameters: a contribution to the ephemeris rotation error Montenbruck
- Liu, Yue & Liu, Fei & Gao, Yang & Zhao, Lin. (2018). Implementation and Analysis of Tightly Coupled Global Navigation Satellite System Precise Point Positioning/Inertial Navigation System (GNSS PPP/IMU) with IMU sufficient Satellites for Land Vehicle Navigation. Sensors. 18. 4305. 10.3390/s18124305.
- Mayer-Guerr, T., Behzadpour, S., Eicker, A., Ellmer, M., Koch, B., Krauss, S., Pock, C., Rieser, D., Strasser, S., Suesser-Rechberger, B., Zehentner, N., Kvas, A. (2021). GROOPS: A software toolkit for gravity field recovery and GNSS processing. Computers & Geosciences, 104864. <https://doi.org/10.1016/j.cageo.2021.104864>
- Montenbruck O, Steigenberger P, Hauschlid A (2014) Broadcast versus precise ephemerides: a multi-GNSS perspective, GPS Solutions
- Liu T, Chen H, Jiang Weiping (2022) Assessing the exchanging satellite attitude quaternions from CNES/CLS and their application in the deep eclipse season, GPS Solutions 26(1)
- Montenbruck O, Steigenberger P (2024) The 2024 GPS accuracy improvement initiatives, GPS Solutions
- Montenbruck O, Steigenberger P, Hauschlid A (2014) Broadcast versus precise ephemerides: a multi-GNSS perspective, GPS Solutions
- Montenbruck O, Hauschlid A (2014 a) Differential Code Bias Estimation using Multi-GNSS Observations and Global Ionosphere Maps, ION
- Montenbruck, O., Schmid, R., Mercier, F., Steigenberger, P., Noll, C., Fatkulin, R., Kogure, S. & Ganeshan, A.S. (2015) GNSS satellite geometry and attitude models. Advances in Space Research 56(6), 1015-1029. DOI: 10.1016/j.asr.2015.06.019
- Niu, Z.; Li, G.; Guo, F.; Shuai, Q.; Zhu, B (2022) An Algorithm to Assist the Robust Filter for Tightly Coupled RTK/IMU Navigation System. *Remote Sens.* **2022**, *14*, 2449. <https://doi.org/10.3390/rs14102449>
- Schmidt, G, Phillips, R (2010) IMU/ GPS Integration Architecture Performance Comparisons. NATO.
- Steigenberger P, Montenbruck O, Bradke M, Ramatschi M (2022) Evaluation of earth rotation parameters from modernized GNSS navigation messages, GPS Solutions 26(2)
- Strasser S (2022) Reprocessing Multiple GNSS Constellations and a Global Station Network from 1994 to 2020 with the Raw Observation

Approach, PhD Thesis, Graz University of Technology

Suvorkin, V., Garcia-Fernandez, M., González-Casado, G., Li, M., & Rovira-García, A. (2024). Assessment of Noise of MEMS IMU Sensors of Different Grades for GNSS/IMU Navigation. *Sensors*, 24(6), 1953. <https://doi.org/10.3390/s24061953>

Sylvain L, Banville S, Geng J, Strasser S (2021) Exchanging satellite attitude quaternions for improved GNSS data processing consistency, Vol 68, Issue 6, pages 2441-2452

Tanil, Cagatay & Khanafseh, Samer & Pervan, Boris. (2016). An IMU Monitor for GNSS Spoofing Attacks during GBAS and SBAS-assisted Aircraft Landing Approaches. 10.33012/2016.14779.

Walter T, Blanch J, Gunning K (2019) Standards for ARAIM ISM Data Analysis, ION

Wang, C & Jan, S (2025). Performance Analysis of MADOCA-Enhanced Tightly Coupled PPP/IMU. NAVIGATION: Journal of the IMUtitute of Navigation March 2025, 72 (1) navi.678; DOI: <https://doi.org/10.33012/navi.678>

Wang N, Li Z, Montenbruck O, Tang C (2019) Quality assessment of GPS, Galileo and BeiDou-2/3 satellite broadcast group delays, Advances in Space Research

Wang J, Huang S, Lia C (2014) Time and Frequency Transfer System Using GNSS Receiver, Asia-Pacific Radio Science, Vol 49, Issue 12

<https://cggts-analyser.streamlit.app>

Yang N, Xu A, Xu Z, Xu Y, Tang L, Li J, Zhu H (2025) Effect of WHU/GFZ/CODE satellite attitude quaternion products on the GNSS kinematic PPP during the eclipse season, Advances in Space Research, Volume 75, Issue 1,

Note: References in this list might also include references provided to previous issues.


Data sources and Tools:

<https://cddis.nasa.gov> (Daily BRDC); http://ftp.aiub.unibe.ch/CODE_MGEX/CODE/ (Precise Products); BKG “SSRC00BKG” stream; IERS C04 ERP files

(The monitoring is based on following signals- GPS: LNAV, GAL: FNAV, BDS: CNAV-1, QZSS:LNAV IRNSS:LNAV GLO:LNAV (FDMA))

Time Transfer Through GNSS Pseudorange Measurements: <https://e-learning.bipm.org/login/index.php>

Allan Tools, <https://pypi.org/project/AllanTools/>

gLAB GNSS, <https://gage.upc.edu/en/learning-materials/software-tools/glab-tool-suite>. 

There's Fungus Among Us. But Where Exactly?

The world's biological riches are not evenly distributed. Instead, much of Earth's plant and animal life is concentrated in a small number of biodiversity hot spots — from the tropical rainforests of the Amazon to the alpine meadows of the Himalayas — that have earned enormous scientific and conservation attention.

Now, new research suggests that more of these critical hot spots could be hiding beneath our feet

— undocumented and largely unprotected.

Recently, an international team of scientists unveiled a global underground atlas, mapping the biodiversity of organisms known as mycorrhizal fungi. The fungi, which live in and on plant roots, form vast underground networks and perform critical ecosystem services, transporting nutrients to plants, storing carbon, bolstering soil health and helping crops survive

environmental shocks and stresses.

Using machine learning models, the scientists predicted that rich reservoirs of these fungi lie hidden in some unexpected places, including the Alaskan tundra and Mediterranean woodlands and scrublands. The dense Amazonian jungle did not stand out as a fungal biodiversity hot spot, but the neighboring savanna, the Brazilian Cerrado, did.

“The Amazon of the underground is not actually in the Amazon rainforest,” said Michael Van Nuland, the lead data scientist at the Society for the Protection of Underground Networks, a research organization that led the mapping effort. “These patterns of diversity that we’re seeing are unique.”

Alarming, they found, relatively few of these critical hot spots are in ecologically protected areas.

The scientists say that more work is needed to confirm their predictions, which were published in the journal *Nature*, and to elucidate how these fungi function. But the scientists hope that the findings will usher in a more expansive view of biodiversity and conservation.

“This paper is wildly exciting,” said Rebecca Shaw, the chief scientist at the World Wildlife

Fund, who was not an author of the study. “We’ve been studying aboveground biodiversity and its functioning for things that we care about — like water retention, carbon sequestration, productivity — for five decades. But we’ve made very little progress doing the same thing with belowground biodiversity.”

She added, “I’ll be looking to this group in the future to help me better understand: What do we protect?”

More than 80 percent of the world’s plants form symbiotic relationships with mycorrhizal fungi, which entwine themselves in the plants’ roots and spread thin filaments underground. But the fungi, which are often invisible to the naked eye, have not traditionally been well studied.

“We really had this aboveground bias, I think, as a society,” said Toby Kiers, an

evolutionary biologist at the Free University of Amsterdam who co-founded SPUN (Society for The Protection of Underground Networks) and serves as its executive director. “How do we protect what we can’t see?”

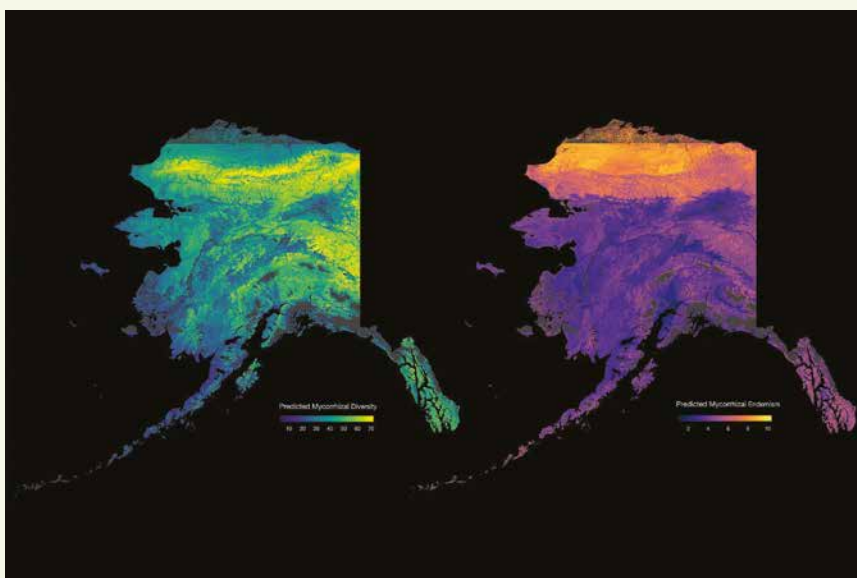
Genomic sequencing has provided a new tool, allowing scientists to identify mycorrhizal fungi by sequencing the DNA present in soil samples collected across the world.

In the new study, the researchers mined several large global repositories of this fungal data, pulling together more than 2.8 billion fungal DNA sequences from 25,000 soil samples collected in 130 countries. They built machine-learning models to analyze this data, alongside a variety of environmental variables, such as the climate and elevation at each collection site.

The models then made predictions about fungal biodiversity across the entire planet, estimating both richness — how many species were present at a given location — and rarity, or how unique those fungi were.

“If we go to a place like Mongolia, are there really unique fungi that have unique traits that could be very helpful in the future?” Dr. Kiers said. “Are there fungi that have evolved a very high tolerance to salt or to drought?”

Some of the findings mirror other well-documented




An example From SPUN's Underground Atlas showing predicted patterns of ectomycorrhizal biodiversity (left) and endemism (right) across underground ecosystems. Bright colours indicate higher richness and endemism. SPUN

biodiversity trends. For instance, the map predicts that the biodiversity of one major subgroup of mycorrhizal fungi — associated with grasses, crops and many species of trees — is greatest near the Equator, a pattern that holds for many plants and animals. (Specific hot spots for these fungi included the Brazilian savanna and tropical forests in Southeast Asia and West Africa.)

But the opposite was true for another subgroup of mycorrhizal fungi that is associated with a select group of trees, including pines, spruces and oaks. The richness of these mycorrhizal fungi was highest closer to the poles, with hot spots that included forests in Siberia, Canada and the United States. And tundras — cold, dry habitats — were brimming with rare species of these fungi.

Indeed, extreme climates and isolated habitats, like mountaintops, seem to harbor more rare fungi, Dr. Kiers said. Preliminary data suggest that deserts may also serve as these kinds of hot spots, she added.

The researchers also found that just 10 percent of the predicted richness hot spots, and 23 percent of the rarity ones, were located in protected areas, potentially leaving them at risk. **“It puts a number to what we’ve been saying for a while — that these are underappreciated systems or underappreciated organisms on the planet,”** Dr. Van Nuland said.

<https://www.nytimes.com/2025/07/23/science/fungus-spun-atlas-mychorrhizal.html> 

Galileo OSNMA is now fully operational

The European Union Agency for the Space Programme has officially declared its Galileo Open Service Navigation Message Authentication (OSNMA) initial service fully operational on 24th July 2025. OSNMA introduces a data authentication mechanism for Galileo Open Service users and is available free of charge to Galileo users worldwide. While Galileo satellites have been transmitting OSNMA since 2021 in a test mode, the service lacked formal guarantees. But now OSNMA officially transitions to operational status.

What is OSNMA?

OSNMA enables Galileo satellites to transmit a “digital signature” along with their standard Open Service navigation data. This signature allows receivers to verify that the signal they are receiving genuinely originates from Galileo and not from a malicious or spoofed source. Receivers equipped to fully exploit OSNMA will enjoy significantly improved protection against spoofing attacks.

A Collective European Effort

OSNMA is the result of over a decade of dedicated effort aimed at positioning Galileo at the forefront of satellite navigation. It reflects the strength of collaboration among European institutions and industry. The implementation involves the EU Space Programme Agency (EUSPA), responsible for OSNMA operations via the European GNSS Service Centre in Torrejón, Madrid; the European Space Agency (ESA), which manages the Galileo core infrastructure; and numerous key industrial partners from across the European aerospace sector.

The European Commission’s Directorate-General for Defence Industry and Space (DG DEFIS), and particularly its Satellite Navigation Unit, initiated, conceptualised, and oversees the implementation of OSNMA, and is responsible for overall Galileo Programme Management.

The Canadian Geodetic updates CSRS-PPP service

The Canadian Geodetic Survey (CGS) of Natural Resources Canada (NRCan) updated the Canadian Spatial Reference System Precise Point Positioning (CSRS-PPP) service on 14 May 2025. It includes, for the first time, support for Galileo PPP with ambiguity resolution (Galileo PPP-AR) for E1/E5a observations collected beginning 27 November 2022 when processed with either the Rapid or Final products. Submissions processed with the Ultra-rapid products will continue to support only GPS and GLONASS observations.

The main advantage of including dual-frequency Galileo observations in CSRS-PPP submissions is that they allow users to achieve improved accuracies, especially for shorter datasets, compared with only GPS and GLONASS submissions. This means that users can collect less data to meet their accuracy needs, mainly because, similarly to GPS, CSRS-PPP attempts to fix the integer ambiguities for Galileo when possible.

More details on the CSRS-PPP ambiguity resolution algorithm can be found in the CSRS-PPP version 3 PPPAR tutorial. The addition of Galileo will also improve the satellite geometry, especially when tracking in less-than-ideal conditions. Figures 1 to 3 compare the achievable accuracies between CSRS-PPP v4 with GPS and GLONASS, and CSRS-PPP v5 with GPS, GLONASS, and Galileo, when processing geodetic-quality GNSS observation sets between 15 minutes and 12 hours. The CSRS-PPP v5 accuracy improvement can reach up to 40-60% for datasets of up to one hour and approximately 10-20% for 12 hours. <https://webapp.csrs-scrs.nrcan-rncan.gc.ca>

India plans three more NavIC satellites

India is set to strengthen its homegrown satellite navigation NavIC (Navigation with Indian Constellation) system with the planned launch of three new satellites — NVS-03, NVS-04, and NVS-05 — by 2027, amid concerns over the ageing and partially operational fleet.


According to Union Minister Jitendra Singh, the NVS-03 satellite is scheduled for launch by the end of 2025.

The subsequent satellites, NVS-04 and NVS-05, will be deployed at six-month intervals thereafter, extending the replenishment schedule into 2027. The NavIC system currently comprises 11 satellites launched since inception. [swarajyamag.com](http://www.swarajyamag.com)

DAF sends NTS-3 Vanguard into space on ULA Vulcan rocket

The Department of the Air Force (DAF) launched the Navigation Technology Satellite-3 (NTS-3) Vanguard on the USSF-106 mission from Cape Canaveral Space Force Station, Florida, Aug. 12, 2025. NTS-3 is a payload for the first U.S. national security launch aboard a United Launch Alliance Vulcan rocket.

AFRL designed NTS-3 to provide more robust, resilient and responsive positioning, navigation and timing (PNT) functionality in space, thereby increasing the security and efficacy of PNT systems like GPS.

NTS-3 features a space-based satellite, a ground-based control system and agile user receivers, all linked by reprogrammable software. This allows for rapid, on-orbit or in-the-field updates to all three segments, a significant advancement over previous GPS satellites that required hardware replacements for upgrades. www.afrl.af.mil 

GeoTech Overseas chooses UltraCam Osprey 4.1

GeoTech, a partner of MipMap Holdings, has recently expanded its technological capabilities with the acquisition of Vexcel Imaging's UltraCam Osprey 4.1 aerial camera system. It will support GeoTech's groundbreaking project to create a high-precision Digital Twin of Jeddah, Makkah, Al Ula, NEOM and other cities, covering both urban and surrounding areas. These projects, commissioned by Jeddah Municipality, Makkah Municipality & Royal Commission for Makkah City (RCMC), NEOM, are among the first in the region to use the UltraCam Osprey 4.1, highlighting GeoTech's commitment to innovation and state-of-the-art technology. www.vexcel-imaging.com

China launches remote sensing satellite for Pakistan

China successfully launched a remote sensing satellite for Pakistan aboard a Kuaizhou 1A carrier rocket from the Xichang Satellite Launch Center in Sichuan province. The launch occurred at 10 am local time, with the solid-fueled rocket placing the satellite into its designated orbit. The satellite, designed and manufactured by the Innovation Academy for Microsatellites under the Chinese Academy of Sciences, is intended to bolster land resource management as well as disaster prevention and mitigation, according to China Aerospace Science and Industry Corp (CASIC), which developed the Kuaizhou rocket. www.spacedaily.com

First lunar exploration mission of TASA

The Taiwan Space Agency (TASA) has announced plans for its first lunar exploration mission and collaboration with international space agencies to integrate two scientific payloads, developed jointly by the TASA and academia, into a lunar lander. The project is slated for launch as early as 2028 and will research the lunar mini-magnetosphere and vortex regions, as well as topography and ultraviolet astronomy. In response to rapidly evolving space industry trends, Taiwan's third phase of the National Space Science and Technology Development Plan is undergoing budget increases and


timeline extensions. According to the TASA, flight and engineering components of its two major mission payloads, the Lunar Vector Magnetometer and the Formosa Lunar Ultraviolet Telescope Experiment (FLUTE), will be ready by the end of this year. www.rti.org.tw

China launches drone ship to recover reusable rockets

China has launched its first drone ship to recover reusable rockets – becoming only the second country after the United States to master the technology – as Beijing pushes forward with its ambitious space programme. The launch of the new vessel marks a major step forward for China's push to develop reusable rockets – a technology seen as vital to helping the country cut the cost of space travel and develop a commercial space industry. The new vessel – named the Xingji Guihang, or “Interstellar Return” – was developed by the Beijing-based private aerospace firm iSpace, and it will eventually be used to recover reusable rockets developed by several Chinese manufacturers. www.scmp.com

UAE Space Agency launches Emirati space leadership program

The UAE Space Agency, through its National Space Academy initiative, has launched the Space Mission and Satellite Engineering Program (SMSE) in partnership with EDGE Group. The program is designed to develop a new generation of Emirati professionals equipped to drive the nation's expanding space ambitions. Delivered in collaboration with EDGE subsidiaries FADA and BEACON RED, the initiative offers specialized, hands-on training in space mission design, satellite engineering, and mission operations.

It targets Emirati professionals, STEM researchers, and recent graduates, providing advanced technical knowledge and practical experience to prepare them for leadership roles in space-related fields. Running from September to November 2025, the ten-week course will be held across multiple locations, including the UAE Space Agency, BEACON RED's training center, and FADA's facilities. fastcompany.me.com 

New remote-sensing system maps Antarctic vegetation

Queensland University of Technology (QUT) researchers have developed an advanced remote sensing method for accurately detecting and mapping Antarctica's delicate moss and lichen growth, the mainstays of the continent's fragile ecosystems.

The research team also developed a way to survey Antarctica's vegetation that is non-invasive and will enable accurate surveys more quickly and cheaply than before.

First author and research fellow Dr Juan Sandino from QUT's School of Electrical Engineering & Robotics described mosses and lichens as the green "stress barometers" of Antarctica.

Dr Sandino said the researchers flew a UAV (Uncrewed Aerial Vehicle)-mounted hyperspectral camera, which records hundreds of colours for every pixel, combined with Global Navigation Satellite System Real-Time Kinematic (GNSS-RTK) to precisely anchor every pixel to its exact location. High-resolution RGB UAV imagery was also captured to provide a familiar visual context.

The researchers compared 12 different AI models for labelling the vegetation and the best options reached about 99 per cent accuracy while staying consistent in rigorous tests.

The research is part of the \$36 million ARC-funded Securing Antarctica's

Environmental Future (SAEF) program through a dedicated six-year, \$1.8million project, and is codirected by Professor Felipe Gonzalez and Professor Barbara Bollard from the University of Wollongong. www.qut.edu.au



Developing neo magnets for drones

ePropelled, Inc. has signed a joint development agreement (JDA) with USA Rare Earth, Inc. (USAR) to develop a strategic supply and purchase relationship providing sintered neo magnets for use in ePropelled's state-of-the-art motors, which are used in a multitude of uncrewed air, land, and sea vehicles (commonly referred to as drones).

Sintered magnet technology, specifically developed for high-performance permanent magnets, involves precision processing of rare earth alloys to deliver unmatched magnetic strength and stability. USAR will immediately begin prototyping neo magnets for use in ePropelled's high-performance motors, controllers, generators, and power management systems from its Oklahoma manufacturing plant. ePropelled.com.

GöKHUN tactical UAS designed for land and sea missions

The GöKHUN unmanned aerial system (UAS) from Turkish company ESEN is a tactical vertical take-off and landing (VTOL) drone system that does not require a runway, offering maximum flexibility in operational use. It combines the compact mobility of a NATO Class I UAV with the performance data of a Class II tactical system. www.esensi.com.tr

Exail to deliver 100 navigation systems for U.S. defense UUVs

Exail has signed a contract to supply 100 Phins compact inertial navigation systems (INS) to a U.S.-based global defense company for use in unmanned underwater vehicles (UUVs). The Phins Compact INS is designed to provide precise navigation capabilities in challenging environments, remaining functional even when external signals are disrupted. The system's compact design enables rapid integration into UUVs, allowing for flexible and efficient mission operations in dynamic maritime settings. www.exail.com

JAVAD GNSS News

Collaboration with Inertial Labs

JAVAD GNSS and Inertial Labs, Inc. have announced a strategic collaboration that integrates Inertial Labs' industry-recognized IMU-P modules with JAVAD's advanced OEM GNSS receivers. The result is a next-generation GNSS+INS platform. At the heart of this innovation is the JAVAD TR-3Si, a receiver purpose-built for seamless integration with professional IMU modules. Paired with the advanced IMU-P, the system delivers unparalleled accuracy and stability, providing mission-critical performance across aerospace, defense, autonomous systems, UAVs, robotics, precision agriculture, and other demanding applications. www.javad.com

New data collection software

The latest data collection software - Javad Data Collector (JDC) interfaces effortlessly with the company's modern line of smart antennas. It features simple, intuitive workflows that require minimal training, making it accessible for users of all skill levels. The software includes a Signal Bar for a quick view of receiver status, ensuring users can easily monitor their equipment's performance. www.javad.com

CompassAVL launched

CompassAVL tracks snowplowing, sweeping, solid waste removal, maintenance and other fleet operations. Automatic privacy filters remove sensitive locations using geofenced zones and exclude idling or parked vehicles. The system's live GPS viewer integrated with Esri® ArcGIS basemaps displays routes and shows real-time vehicle telematics to keep citizens and staff informed, while enhancing driver safety. www.compasscom.com

Trimble RTX-NMA introduced

Trimble RTX-NMA (Navigation Message Authentication) is the first solution on the market to mitigate spoofing

attacks on the GPS and BeiDou satellite constellations. It leverages the Trimble RTX correction service and enhances the security and integrity of GNSS navigation messages for all Trimble ProPoint receivers. Used in conjunction with Galileo OSNMA, Trimble customers now have three constellations protected from spoofing attacks.

Trimble RTX-NMA seeks to detect both fake GNSS signals and faulty ephemeris data through real-time authentication that ensures navigation messages from multiple RTX reference station receivers are genuine and trustworthy. It also encompasses faulty ephemeris detection, preventing unreliable data from being included in the correction stream. www.trimble.com

GMV strengthens its commitment with COVE

GMV is working with the Space Surveillance and Operations Center (COVE) as part of a Real-World Event (RWE) within the framework of Global Sentinel, by providing support and capabilities for the operational tracking of the Spanish satellite Spainsat NG1.

GMV has once again provided technical support to the COVE of the Spanish Space Command (MESPA), part of the Spanish Air and Space Force (EA), during the RWE held from August 3 to 7 as part of the Global Sentinel international military initiative. For the first time, the event was coordinated and led internationally by COVE and was focused on the operational tracking of the Spanish satellite Spainsat NG1 and its relocation maneuvers toward its final geostationary orbit. The scenario involved international cooperation in space defense, with contributions from the space commands of France, Italy, Japan, Romania, and Ukraine. gmv.com

Septentrio teams up with Gateworks

Septentrio is collaborating with Gateworks Corporation, which is now bringing its first Septentrio-based product to market, a new

M.2 card called GW16160, which provides reliable high-accuracy positioning powered by the mosaic-X5 GNSS module. Designed and manufactured in the USA, the GW16160 allows engineers to integrate high-accuracy GNSS into edge systems without bulky external receivers or complex RF design. This ultra-low power card features an M.2 A/E-Key interface with USB 2.0 connectivity for plug-and-play integration. septentrio.com

Mapping deep mine without GNSS or infrastructure

Advanced Navigation has successfully demonstrated a breakthrough in underground navigation, delivering high-precision positioning without reliance on fixed infrastructure or GNSS, in Europe's deepest underground mine in Pyhäjärvi, Finland.

The Hybrid Navigation System, combining a Laser Velocity Sensor (LVS) with the Boreas D90 fiber-optic gyroscope (FOG) Inertial Navigation System (INS), achieved consistent sub-0.1% navigation error across multiple runs, without relying on any fixed positioning infrastructure, pre-existing maps, or external aiding.

Navigating the vast subterranean network of the Pyhäsalmi Mine poses significant challenges. Located 1.4 km underground with a 63 degree latitude – just two degrees below the Arctic Circle, where traditional systems fail – the mine is completely impervious to GNSS signals. Its repetitive, multi-level tunnel network creates a high risk of visual disorientation, while its metallic ores distort magnetic fields and scatter radio waves.

To maintain and enhance this accuracy, the INS is fused with Advanced Navigation's LVS. Using infrared lasers, LVS continuously measures the vehicle's true 3D velocity relative to the ground. This real-time data is critical for correcting the gradual 'drift' that occurs in standalone inertial systems, enabling the Hybrid System to maintain precision over extended distances. www.advancednavigation.com

Value Line steering for small farms by Topcon

Topcon Agriculture has released its new Value Line Steering solution for farmers using mid-range tractors on small- to medium-sized farms. It represents a significant step in making autosteering technology, typically used on larger machinery, accessible to a broader range of farmers.

The new solution is a comprehensive package that includes a GNSS receiver, electric steering wheel controller, touchscreen console and Horizon Lite software, compatible with front-wheel-steer tractors. Farmers also have the option to add local, satellite or RTK correction services such as Topcon's Topnet Live for enhanced precision based on their unique needs. www.topconpositioning.com

NextNav, Oscilloquartz partnership

NextNav and Oscilloquartz have partnered to demonstrate how 5G-powered terrestrial PNT technology combined with Oscilloquartz's established synchronization systems can serve as a scalable complement and backup to GPS. The initiative aims to maintain the operation of critical infrastructure, such as data centers, utilities, and emergency services, during GPS outages by distributing precise, coordinated universal time (UTC) over existing 5G networks for both indoor and outdoor environments.

The collaboration integrates Oscilloquartz's synchronization technology with NextNav's terrestrial 5G PNT platforms to introduce an additional timing source, thereby reducing end-user dependence on GPS alone. www.oscilloquartz.com

NAL Research, partners launch Iridium-based tracking

NAL Research is partnering with SGM Technology, a maritime technology company, and Tschudi Shipping, a maritime logistics company, to deliver a resilient navigation and tracking

SUBSCRIPTION FORM

YES! I want my **Coordinates**

I would like to subscribe for (tick one)

☐ 1 year ☐ 2 years ☐ 3 years

12 issues

24 issues

36 issues

Rs.1800/US\$140

Rs.3400/US\$200

Rs.4900/US\$300

*

**SUPER
saver**

First name

Last name

Designation

Organization

Address

.....

City Pincode

State Country

Phone

Fax

Email

I enclose cheque no.

drawn on

date towards subscription

charges for Coordinates magazine

in favour of 'Coordinates Media Pvt. Ltd.'

Sign Date

Mail this form with payment to:

Coordinates

A 002, Mansara Apartments

C 9, Vasundhara Enclave

Delhi 110 096, India.

If you'd like an invoice before sending your payment, you may either send us this completed subscription form or send us a request for an invoice at iwant@mycoordinates.org

* Postage and handling charges extra.

MARK YOUR CALENDAR

September 2025

IAG Scientific Assembly 2025

1 - 5 September

Rimini, Italy

<https://eventi.unibo.it/iag2025>

Commercial UAV Expo 2025

2 - 4, September

Las Vegas

www.expouav.com

Esri India User Conference 2025

September - Delhi 3rd & 4th, Kolkata 9th,

Hyderabad 10th, Mumbai 12th

www.esri.in

ION GNSS+

08-12 September 2025

Baltimore, USA

www.ion.org

Uncrewed Aerial Vehicles in Geomatics 2025 (UAV-g)

10 - 12 September 2025 Espoo, Finland

<https://uav-g2025.com>

Baška SIF (Spatial Intelligence Forum) Meeting 2025

21 - 24 September 2025

Baška, Krk Island, Croatia

www.visitbaska.hr/en

October 2025

Intergeo 2025

7 - 9 October

Frankfurt, Germany

<https://dvw.de/intergeo/en>

The 8th ISPRS Geospatial Conference

13 - 15 October 2025

Tehran, Iran

<https://geospatialconf2025.ut.ac.ir>

The Arab Conference on Astronomy and Geophysics

13 - 16 October 2025

Cairo, Egypt

<https://acag-conf.org>

The 46th Asian Conference on Remote Sensing

27 - 31 October 2025

Makassar, Indonesia.

<https://acrs2025.mapin.or.id>

3rd MENA Geospatial Forum

29 - 30 October 2025

Riyadh, Saudi Arabia

<https://menageospatialforumksa.com>

November 2025

Canada's National Geomatics Expo 2025

3 - 5 November

Calgary, Canada

<https://gogeomaticsexpo.com>

13th International FIG Workshop on the Land Administration Domain Model & 3D Land Administration

3 - 5 November 2025

Florianópolis, Santa Catarina, Brazil

<https://gdmc.nl>

product line for the commercial shipping industry enabled by Iridium's low-Earth orbit (LEO) satellite network.

NAL Research is a U.S.-based firm specializing in assured PNT solutions. The partnership aims to provide reliable asset tracking and assured navigation in high-risk maritime environments. www.nalresearch.com

Hexagon tech on world's most ambitious road tunnel

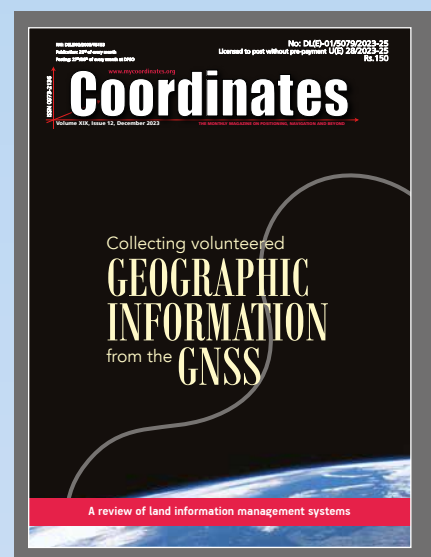
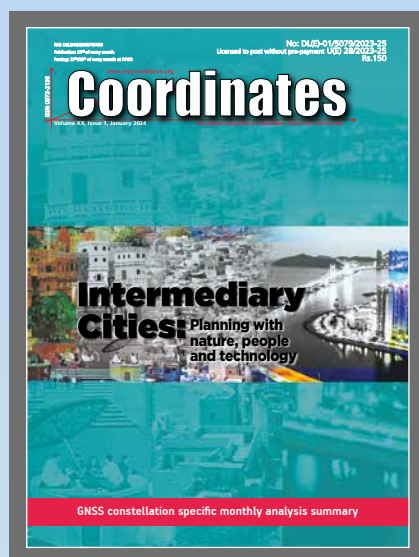
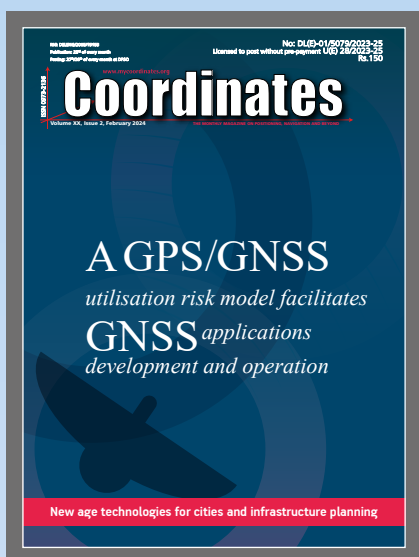
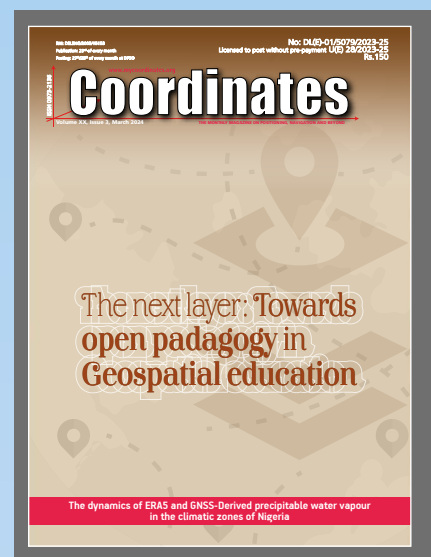
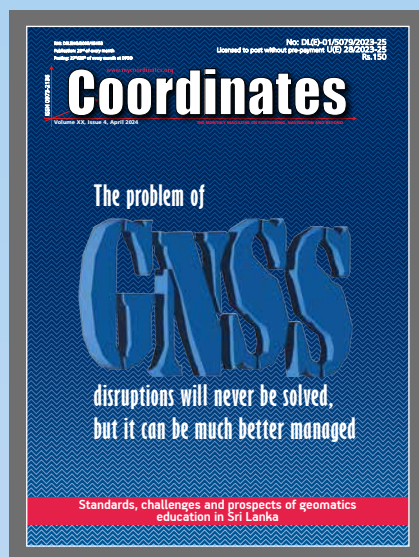
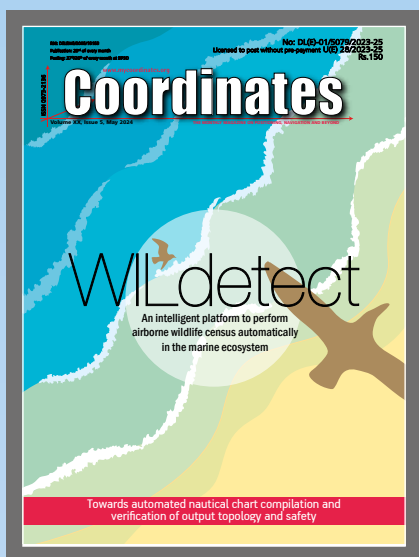
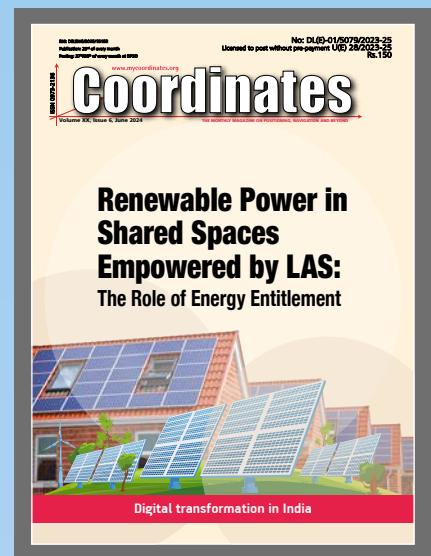
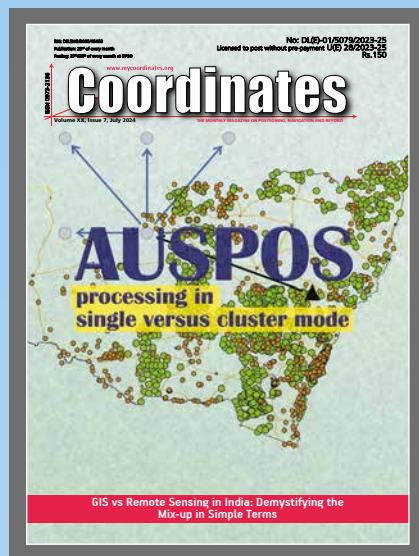
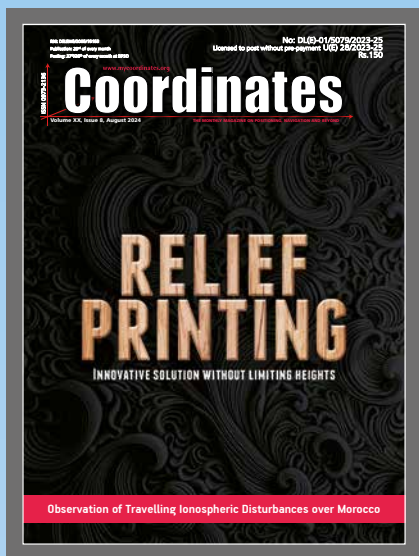
Hexagon is supporting one of the most ambitious infrastructure projects in the world, equipping Skanska with surveying solutions needed to construct Project Rogfast, a 27-kilometre subsea tunnel that will be the longest and deepest of its kind.

Running 392 metres below sea level, the tunnel will connect the cities of Stavanger, Haugesund, and Bergen, helping to cut travel time by 50% and strengthening economic links in the oil and gas sector. Skanska integrates Hexagon's geospatial and construction solutions to deliver the project accurately, safely, and sustainably. hexagon.com

Real-time tracking for safe BVLOS drone deliveries

The Federal Aviation Administration's new Beyond Visual Line of Sight (BVLOS) framework, incorporating Part 108 and Part 146, establishes a regulatory pathway for safe and scalable drone operations. This framework is expected to accelerate the integration of both drone deliveries and air taxis into everyday transportation networks.

Airwayz offers an artificial intelligence-driven unmanned traffic management (UTM) and U-Space Service Provider (USSP) system designed to coordinate multiple drone operators sharing the same airspace. Unlike static management systems, its platform provides fully dynamic airspace allocation and routing, allowing multiple fleets to operate simultaneously without interference. airwayz.co



“The monthly magazine on Positioning, Navigation and Beyond”
Download your copy of Coordinates at www.mycoordinates.org



Motion & Navigation
you can trust

Now compatible*
with



Inertial Navigation Solutions

For Geospatial, Autonomous, & Defense applications:

- High-performance in the smallest package
- Reliable navigation and positioning everywhere
- Post-processing with Q inertia PPK software

*NavIC compatibility: Apogee, Ekinox, Navsight, Quanta series

